THE LARGE–SCALE STRUCTURE OF THE SOLAR WIND *John H. Wolfe*
An invited review

ABSTRACT   The large-scale structure of the solar wind is reviewed on the basis of experimental space measurements acquired over approximately the last decade. The observations cover the fading portion of the last solar cycle up through the maximum of the present cycle. The character of the interplanetary medium is considered from the viewpoint of the temporal behavior of the solar wind over increasingly longer time intervals, the average properties of the various solar wind parameters and their interrelationships. Interplanetary-terrestrial relationships and the expected effects of heliographic latitude and radial distance are briefly discussed.

INTRODUCTION

The purpose of this paper is to review our knowledge of the large-scale structure of the solar wind. This review will be considered from measurements made from 1962 to the present. Results discussed represent data obtained during the fading portion of the last solar cycle (cycle 19) up to approximately the peak of the present cycle. Only proton results will be considered here since they represent the major energy-carrying constituent of the solar wind, and discussions of solar wind composition and solar wind electrons will be covered separately later in the conference. Consideration is given first to the average behavior of the solar wind as observed over many days and up to several solar rotations. The variations in the solar wind are then compared with the large-scale interplanetary magnetic field observations and with the behavior of the solar wind over much longer intervals up through the major portion of a solar cycle. An overall view is given of the average properties of the solar wind, and the interrelationship between solar wind parameters; and interplanetary-terrestrial relationships are discussed along with present speculation of the behavior of the solar wind closer to the sun, far beyond the earth's orbit and at high heliographic latitudes.

The author is at NASA-Ames Research Center, Moffett Field, California.

SHORT-TERM VARIATIONS

Short-term variations are defined here to pertain to the solar wind behavior over periods of days and months, as opposed to years for long term variations. Figure 1 is taken from the Mariner 2 results reported by *Neugebauer and Snyder* [1966] and shows the variation in the solar wind velocity and temperature averaged over 3-hr intervals. The data were taken over approximately 4-1/2 solar rotations in late 1962. One of the most interesting features of these results is the great variability in the solar wind over a time period on the order of days. The velocity is observed to rise frequently from a quiescent value between 300 and 350 km/sec up to as high as approximately 700 km/sec, indicating a high degree of temperature inhomogeneity in the solar corona. Note that these high-velocity streams are often asymmetric, showing a sharper rise in velocity on the leading edge with a slower decay in the descending portion. The temperature is observed to be approximately in phase with the velocity, although frequently tending to high values on the leading edge of the stream somewhat prior to the velocity peak. Although some high-velocity streams tend to persist from one solar rotation to the next, they change in width and amplitude and some streams do not repeat at all. The data thus indicate, at least at the time of the Mariner 2 flight, that dramatic coronal changes take place on a time scale of less than one solar rotation. *Neugebauer and Snyder*
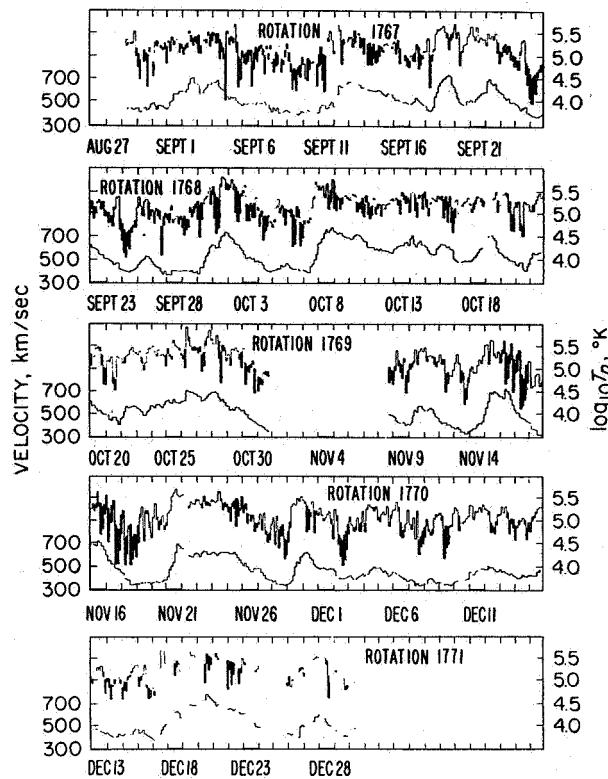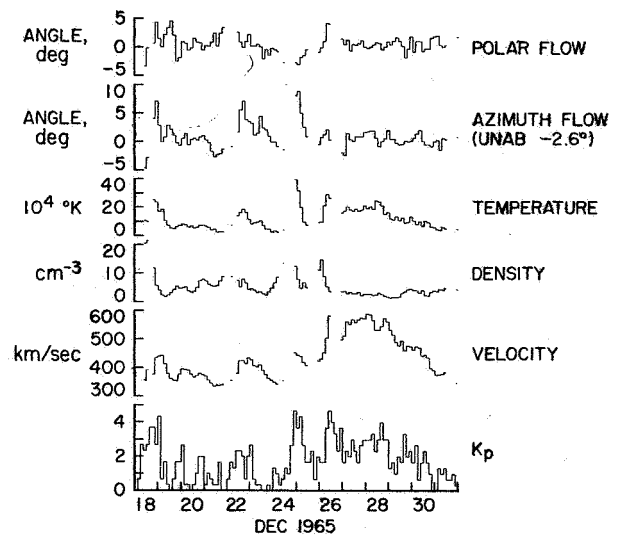
Figure 1. *Three hour average values of velocity and temperature versus time observed by Mariner 2 in late 1962. The time base is chosen to show the 27-day recurrence features associated with solar rotation.*
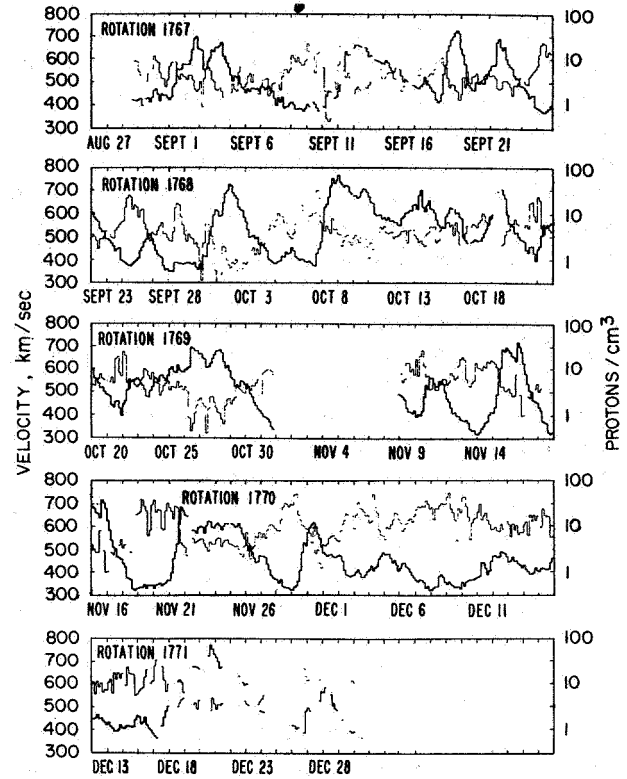
Figure 2. *Mariner 2 3-hr average values of plasma velocity and proton number density versus time.*

[1966] also reported the proton number density for this same period of time as shown in figure 2. For comparison purposes the velocity is again plotted here as the darker curve and the density as the lighter curve. The approximate in-phase relationship between velocity and temperature is in contrast to the striking anticorrelation between velocity and density observed here. In addition to the velocity-density anticorrelation, note also a frequent tendency for large increases in density associated with the leading edge of a high-velocity stream. This density pileup is dramatically observed, for example, in the streams beginning September 1, September 30, and October 7.

Three-hour averages of various solar wind parameters obtained during the last two weeks of December 1965 are shown in figure 3. The data are taken from the Ames Research Center plasma probe on Pioneer 6 [*Wolfe*, 1970] and show the solar wind bulk velocity, proton density and temperature, the two angular components of the flow direction, and the geomagnetic disturbance index K_p. The angular components of the flow direction

Figure 3. *Pioneer 6 3-hr average values of velocity, density, temperature, azimuthal flow direction, polar flow direction and K_p versus time.*

are defined in terms of a spacecraft-centered, solar ecliptic coordinate system. The azimuthal flow direction represents the angle of flow in the ecliptic plane with positive angles defined as flow from the west with respect to the spacecraft-sun line and negative angles from the east. This angle has been corrected for the aberration due to the motion of the spacecraft around the sun and has also been corrected for an apparent systematic error of a negative $2.6°$. The polar flow direction represents the angle of flow in the plane normal to the ecliptic containing the spacecraft-sun line with positive angles defined as flow from the north and negative from the south. As was the case for the Mariner 2 data, the stream structure in the velocity is quite evident in the Pioneer 6 results. The density is observed to pile up in front of the leading portion of the streams with a sharp temperature rise associated with the positive gradient in the velocity. Also note that associated with the leading edge of each stream, the azimuthal flow angle shows that the flow shifts to a direction first from the east and then from the west across the positive gradient in velocity. This is a very persistent stream feature and is even more dramatically observed in figure 4. These data were also obtained from the Pioneer 6 Ames Research Center plasma probe [*Wolfe,* 1970] and show the solar wind bulk velocity and flow directions for the first two weeks of January 1966. Note the one-for-one correlation of the east-west shift in the azimuthal flow direction with the positive gradients in velocity. Although large
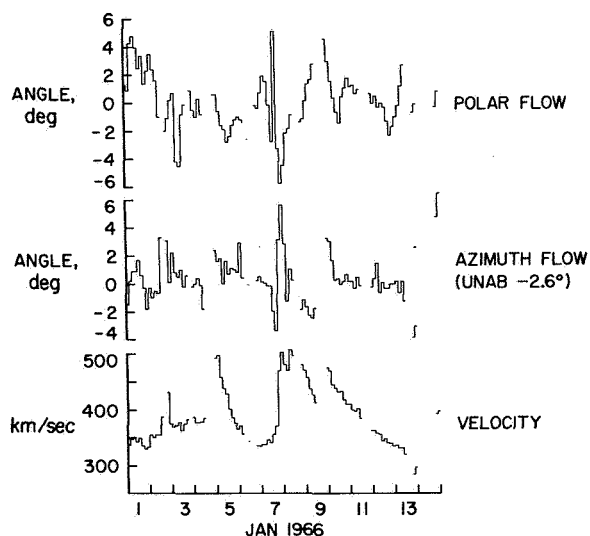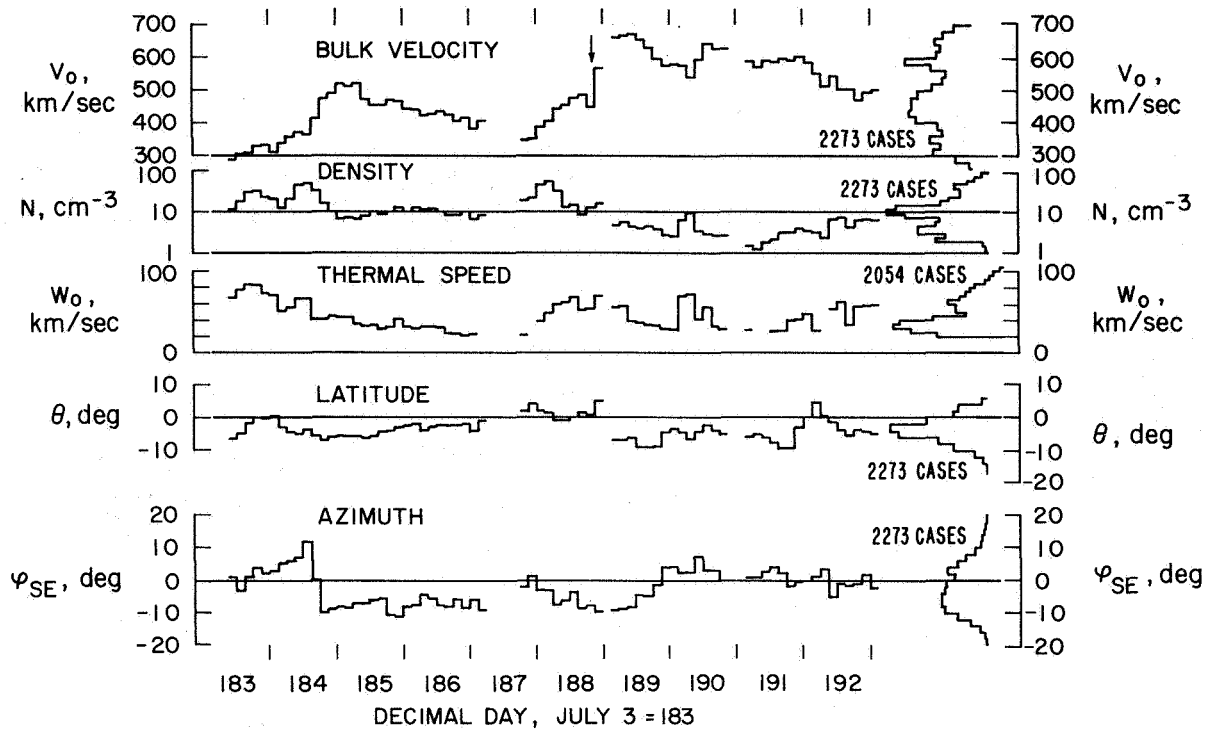
shifts in the polar flow direction are observed, frequently associated with velocity gradients, there is no particular flow pattern discernible in this angular component.

Similar results obtained during the rising portion of the present solar cycle have been reported by *Lyon et al.* [1968] using Explorer 33 data. Figure 5 shows 3-hr average values of the solar wind bulk velocity; density (logarithmic scale); most probable thermal speed, related to temperature by $w = (2kT/m)^{1/2}$; and the azimuthal and latitude (polar) angles. Note that the azimuthal angle φ_{SE}, has been defined here in a sense opposite to that described for figures 3 and 4. The data were taken over the interval July 3-12, 1966. Again, the influence of the solar wind high-velocity stream structure is apparent. Note the striking examples of the density pileup at the leading edges of the high-velocity streams and the east-west shift in azimuthal flow direction across the positive gradient in velocity.

Short-term variations in solar wind behavior as observed over averages of several hours and considered on a time scale of weeks to months appear to be dominated by the solar wind stream structure. Coronal temperature inhomogeneities suggest (as observed near 1 AU) numerous coronal high-temperature regions that give rise to high-velocity solar wind streams; due to the rotation of the sun, these streams interact with the quiescent plasma associated with the ambient coronal solar wind. The stream interactions manifest themselves as a positive gradient in the solar wind convective velocity associated with the leading edge of the stream, which is typically much steeper than the negative gradient in velocity associated with the trailing portion of the stream. Although the velocity and temperature are observed to be approximately in phase, the steep positive gradient in velocity frequently indicates an interaction mechanism for heating the solar wind gas. Although the velocity and density are approximately anticorrelated, anomalous density pileup is frequently observed in association with the leading edge of the stream, presumably because of a "snowplow" effect as high-velocity plasma overtakes the slower ambient gas. Of particular significance is the east-west shift in the azimuthal component of the solar wind flow direction across the positive gradient in bulk velocity associated with the leading edge of the stream. This azimuthal shift in flow direction is consistent with that expected for the azimuthal stresses set up along the average Archimedian spiral of the interplanetary field, the latter presumably defining the interaction geometry between the high velocity plasma stream and the ambient gas. Note that the westward flow shifts at the positive velocity gradients are


Figure 4. *Pioneer 6 3-hr average values of velocity, azimuthal flow direction and polar flow direction versus time.*

Figure 5. *Explorer 33 3-hr averages of azimuthal flow direction, latitude flow direction, thermal speed, proton density and bulk velocity versus time.*

usually of higher amplitude (in angle) than the eastward flow shifts. There also seems to be a frequent tendency for slight eastward flow associated with the more gradual negative gradient in the velocity on the trailing edge of a stream.

SOLAR WIND STREAMS AND MAGNETIC FIELD SECTOR STRUCTURE

Results from the IMP 1 satellite [*Wilcox and Ness,* 1965] indicated the presence of a definite pattern in the dominant polarity of the interplanetary magnetic field. This polarity pattern or sector structure was fairly repetitive over approximately 3 solar rotations observed by the IMP 1 flight. These results are shown in figure 6 where 3-hr averages of the interplanetary magnetic field are plotted starting on November 27, 1963, with the plus symbols representing field lines predominantly outward from the sun and the negative symbols representing field lines predominantly inward toward the sun. The Archimedean spiral lines represent the best-fit sector boundaries separating the different field polarities. The only gross exception to the repeating pattern appears to be the early polarity reversal associated with a geomagnetic storm commencing on December 2, 1963. At the time, *Wilcox and Ness* [1965] attributed this early
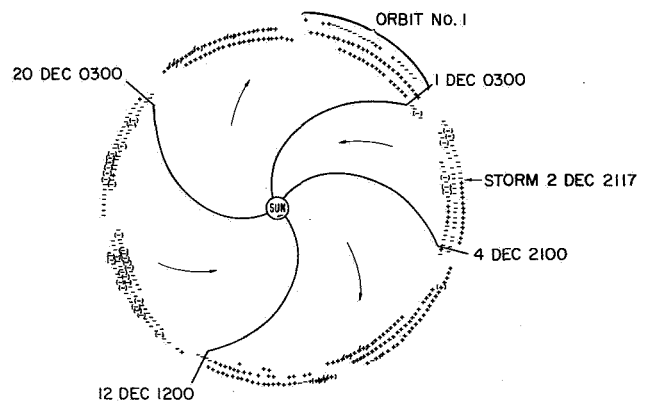
Figure 6. *IMP 1 interplanetary magnetic field sector structure for approximately three solar rotations starting late November 1963. The pluses represent fields predominantly away from the sun and minuses predominantly toward the sun.*

polarity reversal to a higher than expected solar wind velocity associated with the storm.

The obvious next question concerns the relationship between the interplanetary magnetic field sector structure and the high velocity solar wind stream pattern.
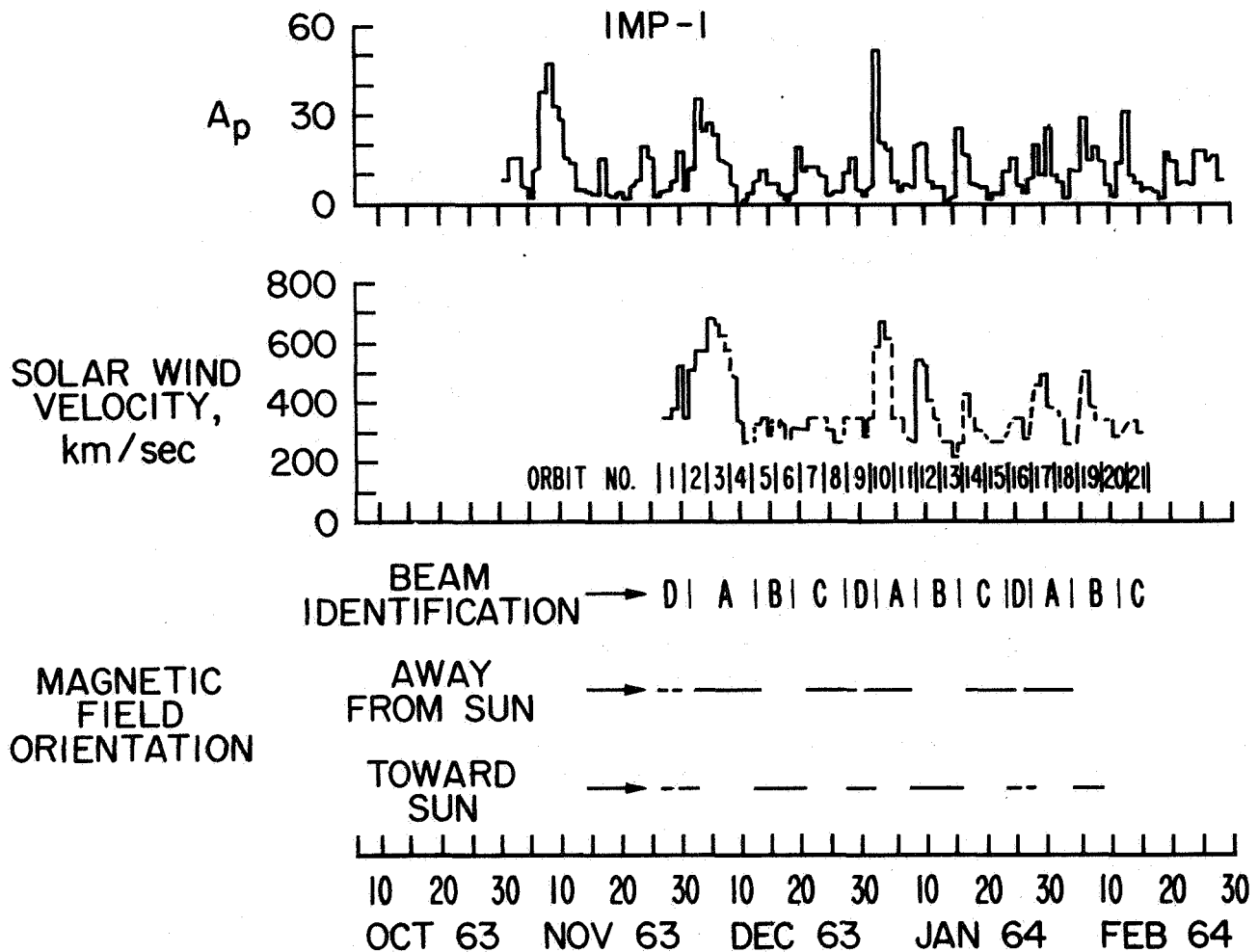
173

IMP-I

A_p 60, 30, 0

SOLAR WIND
VELOCITY,   800, 600, 400, 200, 0
km/sec

ORBIT NO. |1|2|3|4|5|6|7|8|9|10|11|12|13|14|15|16|17|18|19|20|21|

BEAM
IDENTIFICATION ⟶ DI A |BI C IDI A I B I C IDI A I B I C

MAGNETIC
FIELD
ORIENTATION

AWAY
FROM SUN ⟶

TOWARD
SUN ⟶

10 20 30   10 20 30   10 20 30   10 20 30   10 20 30
OCT 63   NOV 63   DEC 63   JAN 64   FEB 64

Figure 7. *Comparison of the IMP 1 solar wind velocity and magnetic field orientation with the A_p index.*

Twenty-four hour average values of the solar wind velocity obtained from the Ames Research Center plasma probe on IMP 1 are shown in figure 7. The dominant orientation of the interplanetary magnetic field is also shown together with the geomagnetic disturbance index A_p. The recurring solar wind streams are identified by letter. The most striking feature is the almost one-for-one correspondence between the solar wind stream pattern and the magnetic field sector structure. Note that the field changes its dominant polarity near the beginning of each stream and that the width of any given stream and corresponding sector are almost identical. If the solar wind streams define the magnetic sector structure, the earlier than expected polarity reversal on December 2, 1963, can be explained in terms of a change in the solar wind stream width on the successive

solar rotation rather than a change in velocity as discussed previously. This can be seen in figure 7, where the stream identified as A has decreased in width by 2 to 3 days between its first observed occurrence to its recurrence on the next solar rotation, whereas the peak velocity has remained near 700 km/sec. It is interesting to note that although the A_p index in general follows the solar wind stream structure, the peak velocity frequently tends to lag the peak in A_p by as much as a day.

Using the method of superposed epoch analysis, *Wilcox and Ness* [1965] compare the interplanetary magnetic field sectors observed by IMP 1 with preliminary MIT plasma data. The results for solar wind velocity are shown in figure 8 where the ordinate is a 3-hr average value of the solar wind velocity and the abscissa is the position within the four large sectors previously

174
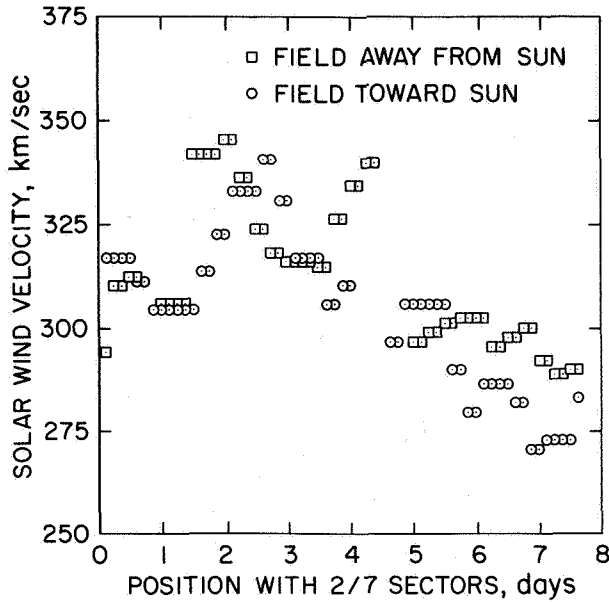
Figure 8. *Superposed epoch analysis of the magnitude of the solar wind velocity as a function of position within the 2/7 sectors shown in figure 6.*

shown in figure 6. Note that both "toward" and "away" sectors are used. It can be seen that the velocity tends to reach a maximum on the order of one fourth to one third of the way through the sector. The second peak near 4 days for the "away" sectors is considered to be an
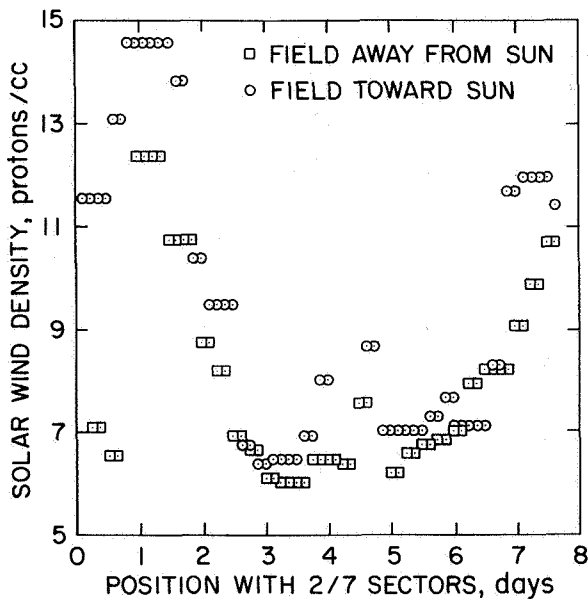
Figure 9. *Superposed epoch analysis of the solar wind density as a function of position within the 2/7 sectors.*

artificial feature related to the perigee passage of the spacecraft near the middle of these "away" sectors. The same analysis was performed for the solar wind density (fig. 9). The density is observed to rise to a maximum value at about one day after the sector beginning, decrease to a minimum near the center, and then rise again at the end of the sector. Note by comparison with figure 8 that the large peak in density at the beginning of the sector coincides with the positive gradient in the velocity, which in turn is associated with the beginning of a new solar wind stream.

Figure 10 shows the sector pattern of the interplanetary magnetic field, as given by *Wilcox and Colburn* [1969], covering the period from the flight of Mariner 2 in 1962 through Explorer 35 in mid-1968. The sector structure is shown overlaying the daily geomagnetic character index C9 with light shading indicating sectors with fields predominantly away from the sun and dark shading for sectors with fields predominantly toward the sun. The diagonal bar indicates an interpolated quasistationary structure during 1964. Although it might be argued that the 1964 interpolations could be misleading, it is certainly clear that the sector structure was much more repetitive from one solar rotation to the next up through the IMP 2 flight as compared to after that time. The period from 1965 through mid-1967 is particularly chaotic with no discernible repeating pattern. This period occurred during the steeply rising portion of the present solar cycle (cycle 20) as compared to near solar minimum for the time of the IMP 1 flight. Note that the sector pattern becomes somewhat more regular in 1968 near solar maximum.

The relationship between the solar wind stream structure and the more chaotic interplanetary magnetic field sector pattern associated with the steeply rising portion of the solar cycle is illustrated in figure 11. The solar wind data are taken from Pioneer 6 [*Wolfe*, 1970] and 24-hr average values of the proton temperature (fitted to an isotropic Maxwellian distribution), number density and velocity have been plotted together with the geomagnetic disturbance index A_p. The data are shown for slightly more than one solar rotation beginning December 18, 1965. The bar graph at the top gives the interplanetary magnetic field sector structure with the extent of the away *(A)* and toward *(T)* sectors as shown. The vertical lines designate the sector boundaries. As was the case for the IMP 1 results discussed earlier, the sector boundaries appear to be associated with the beginning of new solar wind streams. Here, however, more than one stream is observed to appear within a given magnetic sector. The sector commencing on December 25, 1965, for example, is "classic" in that it is quite similar to that
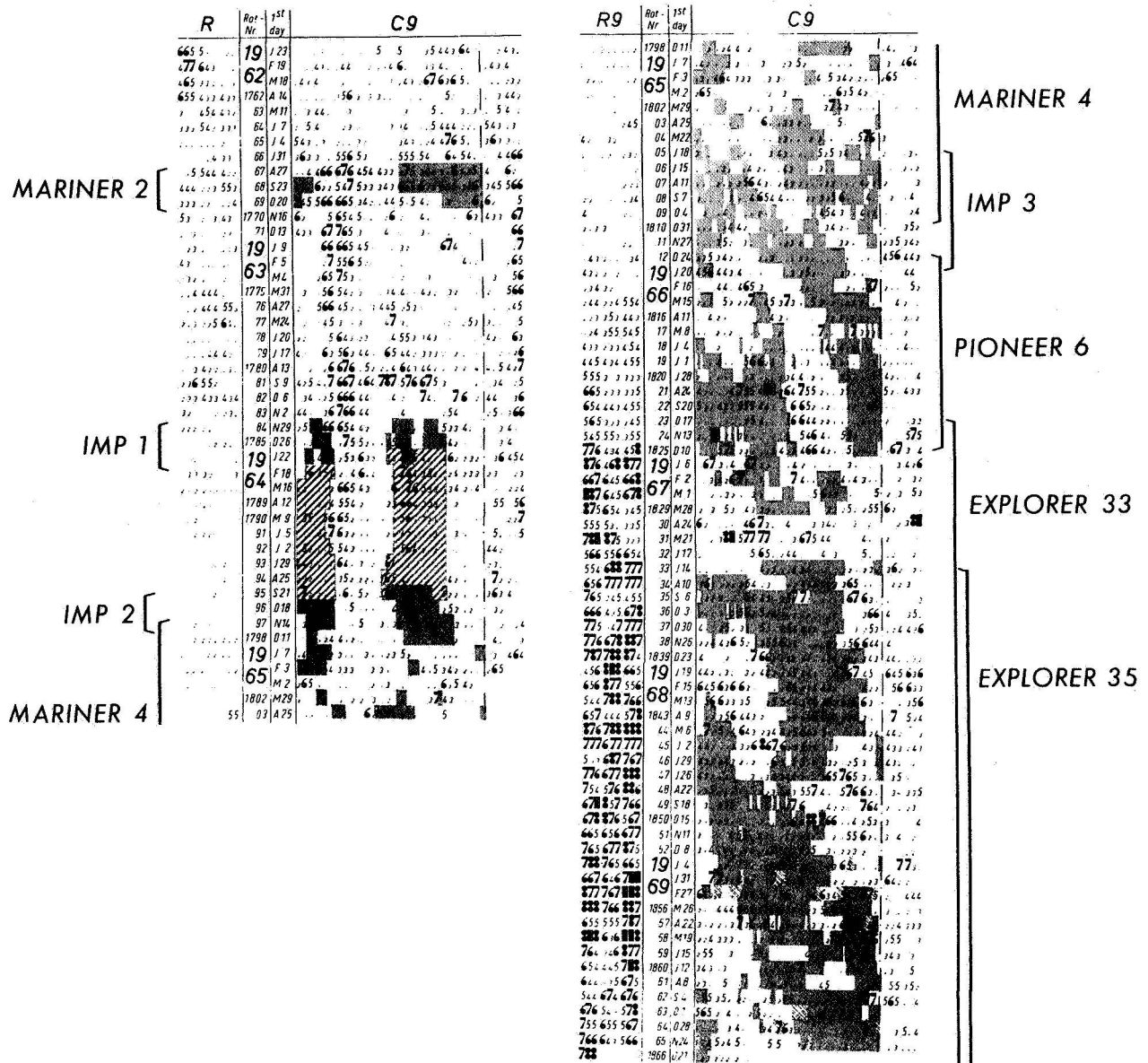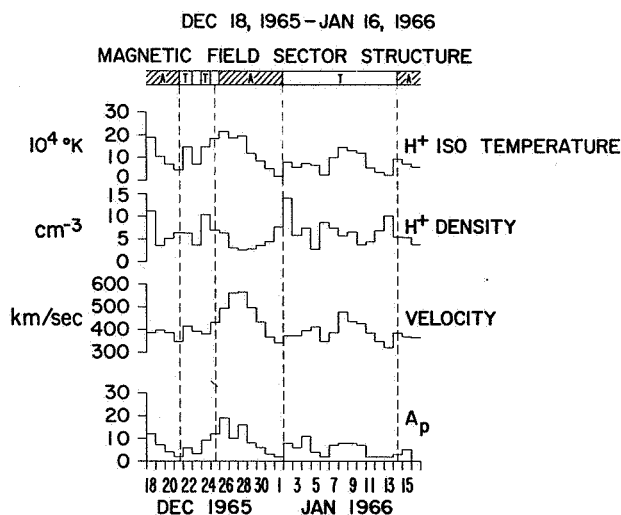
175

MARINER 2

IMP 1

IMP 2

MARINER 4

MARINER 4

IMP 3

PIONEER 6

EXPLORER 33

EXPLORER 35

Figure 10. *Observed sector structure of the interplanetary magnetic field overlaying the daily geomagnetic character index C9. Light shading indicates sectors with field predominantly away from the sun and dark shading indicates sectors with field predominantly toward the sun.*

observed by IMP 1 in late 1963. The velocity is observed to peak approximately one-third of the way through the sector with the density high at the extremes of the sector and at a minimum near the center. In addition, the temperature is seen to peak early in the sector and then descend throughout the remainder of the sector. By contrast, the wide sector beginning January 2, 1966, is seen to contain two distinct solar wind streams. Note, however, that when the sector boundaries do occur, they appear near the beginning of a new solar wind stream.
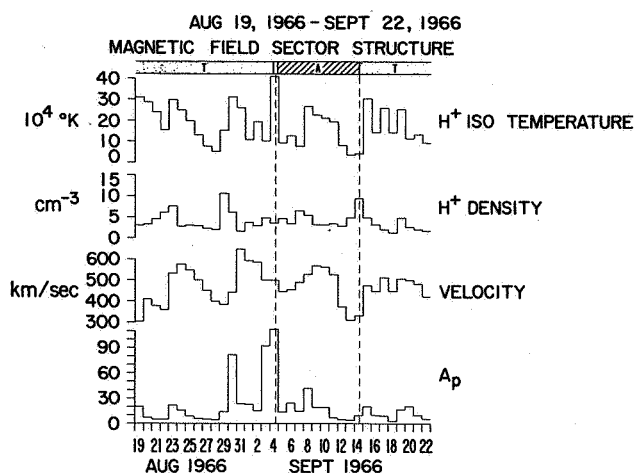
Another interesting feature of the data is the nature of the solar wind streams themselves and their relationship to geomagnetic activity. Although there is general correlation of temperature and anticorrelation of density with velocity, anomalously high densities and temperatures are observed in association with the positive gradients in velocity that define the leading edge of a solar wind stream. With respect to geomagnetic activity, the

176

DEC 18, 1965 - JAN 16, 1966

MAGNETIC FIELD SECTOR STRUCTURE

AUG 19, 1966 - SEPT 22, 1966

MAGNETIC FIELD SECTOR STRUCTURE

Figure 11.   *Pioneer 6 24-hr average values of the solar wind velocity, proton density and temperature plotted versus time. The interplanetary magnetic field sector structure is shown at the top.*

Figure 12.   *Pioneer 7 24-hr average values of the solar wind velocity, proton density and temperature versus time. The interplanetary magnetic field sector structure is shown at the top.*

maximum in velocity tends to lag and the density tends to lead the peaks in the A_p index whereas the temperature appears to be roughly in phase. For the set of data shown here, the correlation coefficient between temperature and A_p was a surprisingly high 0.88. Although not necessarily cause and effect, it seems apparent that the temperature might be a fairly reliable index of the state of disturbance in the solar wind, which in turn determines the level of geomagnetic activity.

A perhaps even more complex example of the relationship between the solar wind streams and the magnetic field sector structure is shown in figure 12. The plots are similar to the previous figure with the solar wind data taken from Pioneer 7 [*Wolfe*, 1970] and are shown for slightly more than one solar rotation beginning August 19, 1966. As was the case with Pioneer 6, more than one solar wind stream is observed within a given magnetic field sector. The sector with field predominantly toward the sun that ends on September 4, 1966, contains three distinct solar wind streams. Note again, however, that when the sector boundaries do occur they appear near the beginning of a new solar wind stream. An exception to this appears to be the September 4, 1966, sector boundary. Investigation of the detailed data [*Wolfe*, 1970] shows, however, that the solar wind stream beginning at this time was somewhat anomalous with a 6-hr "spike" in velocity to values over 530 km/sec associated with this sector boundary. This short-period velocity increase has been washed out in the averaging process in
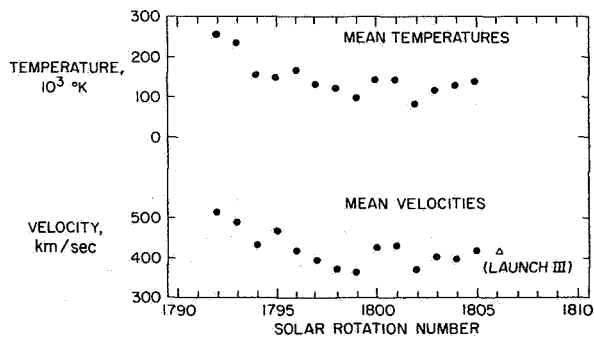
figure 12. The peak in geomagnetic activity on August 30, 1966 illustrates a striking example of the lag, lead and in phase relationship between respectively velocity, density and temperature and the A_p index.

The interplanetary investigations reported thus far clearly indicate an apparent dominance of the magnetic field sector structure by solar wind streaming. The solar wind high velocity streams are apparently the interplanetary manifestations (observed near 1 AU) of coronal temperature inhomogeneities. According to the classical Parker [1958] model, higher temperature regions in the corona would lead to higher interplanetary solar wind velocities. Due to the rotation of the sun, these higher velocity streams would be expected to interact with the lower velocity gas associated with the quiescent corona. Based on the observed interplanetary magnetic field and solar wind characteristics, it is postulated that an interaction region forms along the Archimedean spiral of the interplanetary magnetic field between the high velocity plasma and the lower velocity gas associated with the quiescent corona. For some hypothetical boundary, perhaps associated with the initial velocity increase at the leading edge of a new stream, the leading ambient gas would be accelerated with the loss of kinetic energy (and therefore velocity) for the higher velocity driving gas, giving rise to the observed asymmetry in the stream velocity profile. Because of the essentially infinite conductivity of the medium, the streams cannot penetrate one another, and the plasma density increases forward of

177

this hypothetical boundary in a "snowplow" effect. The observed east-west shift in the solar wind azimuthal flow direction is then simply the reaction of the gas to the tangential stresses set up at the interaction boundary. It is quite likely that waves are generated at this boundary that propagate both upstream and downstream in the moving frame of reference of the gas, giving rise to plasma heating throughout the entire interaction region. Since the interaction region is likely to be the most disturbed, it follows that geomagnetic disturbance indices should correlate with interplanetary solar wind ion temperatures. Since the interaction boundary separates different plasma regimes, the change in the dominant interplanetary magnetic field polarity might be expected to most likely occur at this boundary. Finally, the occurrence of more than one solar wind stream in a given magnetic field sector may be simply due to the greater frequency of coronal temperature inhomogeneities and wider magnetic field sectors associated with increased solar activity as compared to the state of the corona closer to solar minimum.
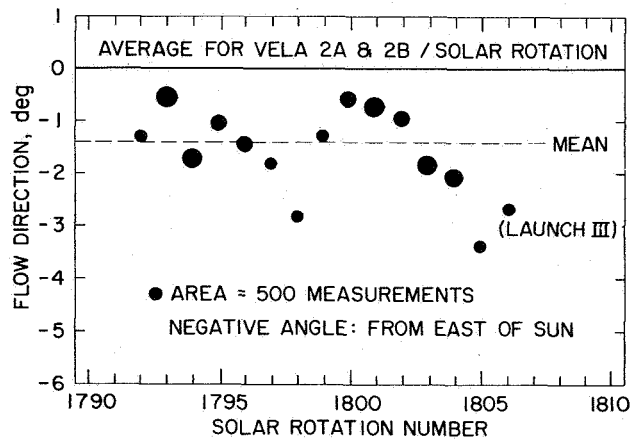
LONG-TERM VARIATIONS

We now consider the long-term variations of solar wind characteristics over many solar rotations during the entire period of solar wind observations from 1962 to the present. Figure 13 shows the solar wind velocities and temperatures averaged over each solar rotation as observed by the Vela 2 satellites [Strong et al., 1967] from July 1964 to July 1965. The last value in the velocity averages was taken from the Vela 3 satellite. This time interval included a solar minimum in October 1964, during solar rotation number 1795. Perhaps the most interesting feature of the data is the great variability of the solar wind parameters over the one year period. The 27-day averages of the solar wind velocity range from

slightly over 500 km/sec for rotation number 1792 to approximately 360 km/sec for rotation number 1799 for an overall variation of roughly 140 percent. Similarly, the temperature ranges from approximately 2.6×10^5 °K for rotation number 1792 to about 9×10^4 °K for rotation number 1802 for an overall variation of almost a factor of 3. It is enticing to speculate that the decline in temperature and velocity from rotation 1792 to 1799 is associated with the decline in solar activity. It should be pointed out, however, that the actual minimum in the sunspot number occurred during rotation number 1795 (October 1964), and the geomagnetic activity in July 1964 and October 1964 was about the same. As will be seen later, the total range in solar wind parameters observed here is not significantly different from that observed throughout the entire portion of the solar cycle observed to date.

The variations in the azimuthal flow direction of the solar wind observed by Vela 2 [Strong et al., 1967] over the same time interval is shown in figure 14. The angles have been averaged over each successive solar rotation with the area of each circle representing the statistical weight for each value. The last value was taken from the Vela 3 satellite as indicated. As was the case for velocity and temperature, great variability in the azimuthal flow direction is observed throughout the one-year period. The values of the average azimuthal flow direction range from a minimum of approximately $-0.5°$ for rotation number 1793 to a maximum of approximately $-3.5°$ for

Figure 13. *Solar wind flow speed and proton temperature averaged over solar rotations as measured on the Vela 2 satellites from July 1964 to July 1965.*

Figure 14. *Solar wind flow directions averaged over solar rotations as measured by the Vela 2 satellites from July 1964 to July 1965.*

rotation number 1805. The overall mean value, indicated by the dashed line, was approximately −1.4° indicating a mean azimuthal velocity component of about 10 km/sec. Note that negative angles refer to flow directions from east of the sun.

Using the interplanetary magnetic sector structure results from a variety of satellites and deep space probes, Wilcox and Colburn [1970] have reported the variation in the synodic rotation period of the interplanetary field from 1963 to 1968. The synodic period is plotted in figure 15 with the smoothed sunspot numbers for the present solar cycle and the mean of cycles 1 through 19. Note that synodic period varies from near 27.0 days close to solar minimum up to 28.0 days at the beginning of the solar cycle and then gradually declines back to 27.0 days at solar maximum. Wilcox and Colburn [1970] postulate that the increase from 27.0 to 28.0 days represents the dominance of the interplanetary field by the high solar latitude spot groups associated with the beginning of the solar cycle. The decline in synodic rotation period thereafter is the result of the decrease in latitude of the spot groups as the solar cycle progresses. One might expect then that the synodic period would remain near 27.0 days throughout the remainder of the present solar cycle and not increase until the beginning of the next cycle.
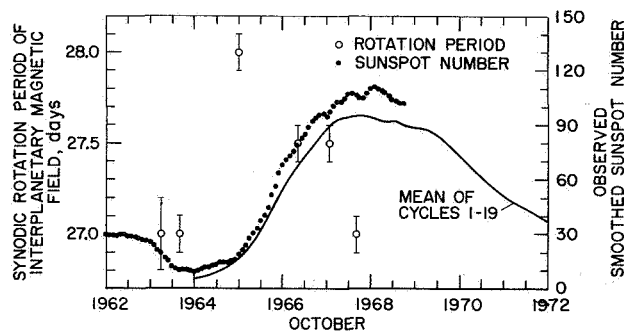
Figure 15. *Synodic rotation period of the interplanetary magnetic field superimposed on the observed smoothed sunspot number from October 1962 to October 1972.*

Table 1 shows selected solar wind parameters reported from the time of Mariner 2 to the present. With respect to the sunspot cycle recalled in figure 15, it is seen that the Mariner 2 observations were obtained during the waning portion of the previous cycle; IMP 2 and Vela 2 observations near solar minimum; Vela 3, Pioneer 6, and Pioneer 7 during the steeply rising portion of the present cycle; Explorer 34 near solar maximum; and finally HEOS 1 slightly past solar maximum. Since the time

Table 1. *Average and most probable values of the various solar wind parameters from all reported spacecraft measurements*

Spacecraft	Institution	V_{mp}, km/sec	V_{AV}, km/sec	N_{mp}, cm^{-3}	N_{AV}, cm^{-3}	T_{mp}, 10^5 °K	T_{AV}, 10^5 °K	ϕ, deg	θ, deg	Approximate date
Mariner 2	JPL		504		5.4		1.5–1.8			9/62 12/62
IMP 1	MIT	330	360	4	7			+1.5		12/63 2/64
IMP 1	ARC		378							12/63 2/64
Vela 2	LASL	325	420			~0.5	1.4	−1.4		7/64 7/65
Vela 3	LASL	~350	400	~4	7.7	~0.4	0.91	−2.5 / −0.9		7/65 7/67
Pioneer 6	MIT		430		6	0.38				12/65 2/66
Pioneer 6	ARC	~340	422	~3.2	5.7	~0.4	1.0	+3.0	+0.56	12/65 2/66
Pioneer 7	MIT		460		6	0.66				8/66 10/66
Pioneer 7	ARC		455	~2.4	4.4	~0.5	1.6	+0.3	+0.34	8/66 10/66
Explorer 34	GSFC	~390	438			0.46				6/67 12/67
HEOS 1	ROME	~390	409	~2	4.3		0.66			12/68 1/70

distributions of velocity, density, and temperature are nongaussian and highly skewed, both the most probable and the average values of these parameters are given in table 1. In addition, the average values (where available) of the components of the flow direction are also given. Here φ is the azimuthal component with positive values for flow from west of the sun and θ is the polar component of the flow with positive values for flow from north of the sun. The most surprising feature of the data is the absence of any definite trend in any of the parameters with respect to the solar cycle. One is tempted to visualize an increase in the average velocity from the time of IMP 1 near solar minimum up through Pioneer 7 during the rising portion of the cycle and then a decline up through solar maximum. Unless there is a significant increase in velocity with declining solar activity (which seems unlikely), the Mariner 2 velocity average is anomalously high. In addition, the Vela 3 velocity average, which includes the entire rising portion of the solar cycle, is anomalously low compared to the Pioneer 6 and Pioneer 7 averages, which were obtained within the time period of the Vela 3 observations. In addition, the Vela 3 averages are anomalously low with respect to the Vela 2 results, which were obtained at solar minimum.

With the possible exception of the angle φ, which is highly susceptible to systematic error, it is hypothesized that the lack of any discernible trend in the various solar wind parameters is primarily due to a sample aliasing problem. It is intended here to consider sample aliasing in a very long term sense. For example, in recalling figure 13, the range in the solar wind velocity averages per solar rotation obtained by Vela 2 for the year period including solar minimum is approximately the same as

179

the range in averages reported by all spacecraft observations for the better part of an entire solar cycle. This surprising result clearly indicates that any effects on the solar wind parameters due to the solar cycle must indeed by subtle compared to the variations observed from one solar rotation to the next regardless of the time of observations within the entire solar cycle. The inevitable conclusion is that the effects of the solar cycle can only be unfolded through continuous monitoring of the interplanetary medium throughout a complete solar cycle.

AVERAGE PROPERTIES

The average properties of the various solar wind parameters are best considered from the point of view of their frequency distributions. Figures 16 through 21 show histograms of solar wind velocity obtained from 7 separate spacecraft observations. Figure 16 was obtained from IMP 1 [*Olbert*, 1968] and covers the time period from December 1963 to February 1964. The velocities shown are 3-hr averages with each bar representing a 20 km/sec velocity interval. Here the most probable velocity was approximately 330 km/sec and the average velocity was 360 km/sec. The velocity histogram shown in figure 17 was obtained from the Vela 2 satellites [*Strong et al.*, 1967] and covers the one-year interval from July 1964 to July 1965. Individual cases have been included here in the velocity intervals shown. The location and widths of the velocity intervals were chosen to coincide with the energy acceptance windows of the Vela 2 plasma analyzers. For these observations, the most probable velocity was approximately 325 km/sec and the average velocity was 420 km/sec. Figure 18 shows the velocity histogram obtained from the Vela 3 measurements [*Hundhausen et al.*, 1970] obtained from July 1965 to November 1967. Here the individual cases are included in 25 km/sec intervals. The Vela 3 results indicate a most probable velocity of approximately 350 km/sec and an average velocity of 400 km/sec. Figure 19 gives the velocity distribution results from Pioneer 6 (lighter curve) from December 1965 to March 1966, and Pioneer 7 (darker curve) from August 1966 to October 1966 [*Mihalov and Wolfe*, 1971]. The velocities given are individual cases included in 10 km/sec intervals. For Pioneer 6 the most probable velocity was approximately 340 km/sec and the average velocity was 422 km/sec. For Pioneer 7 the most probable velocity was not determined and the average velocity was 455 km/sec. The velocity histogram for Explorer 34 [*Burlaga and Ogilvie*, 1970a] is shown in figure 20. The results were obtained
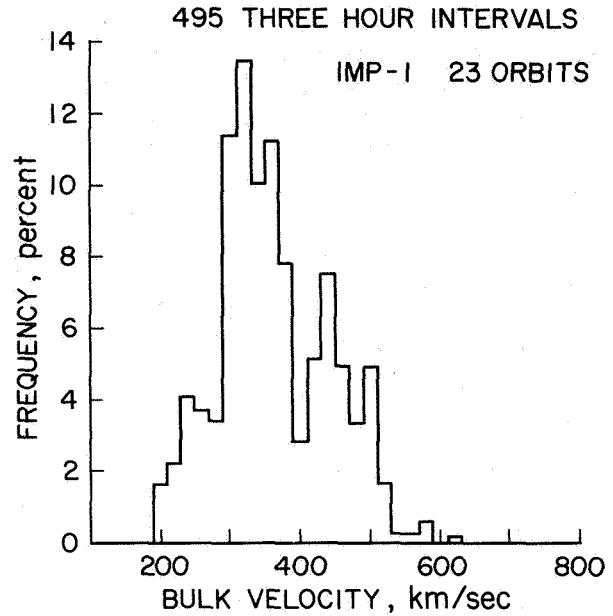

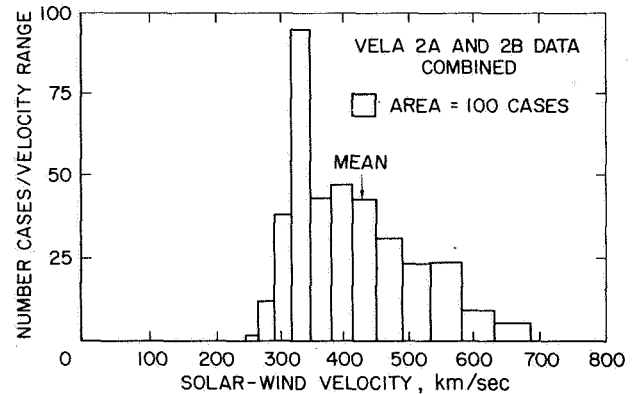Figure 16. *IMP 1 solar wind bulk velocity histogram.*

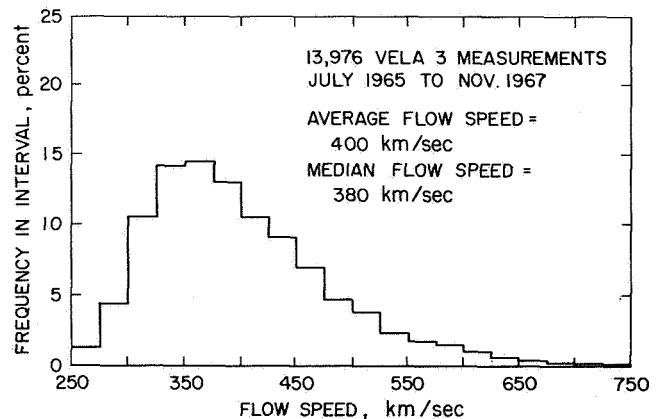Figure 17. *Vela 2 solar wind bulk velocity histogram.*

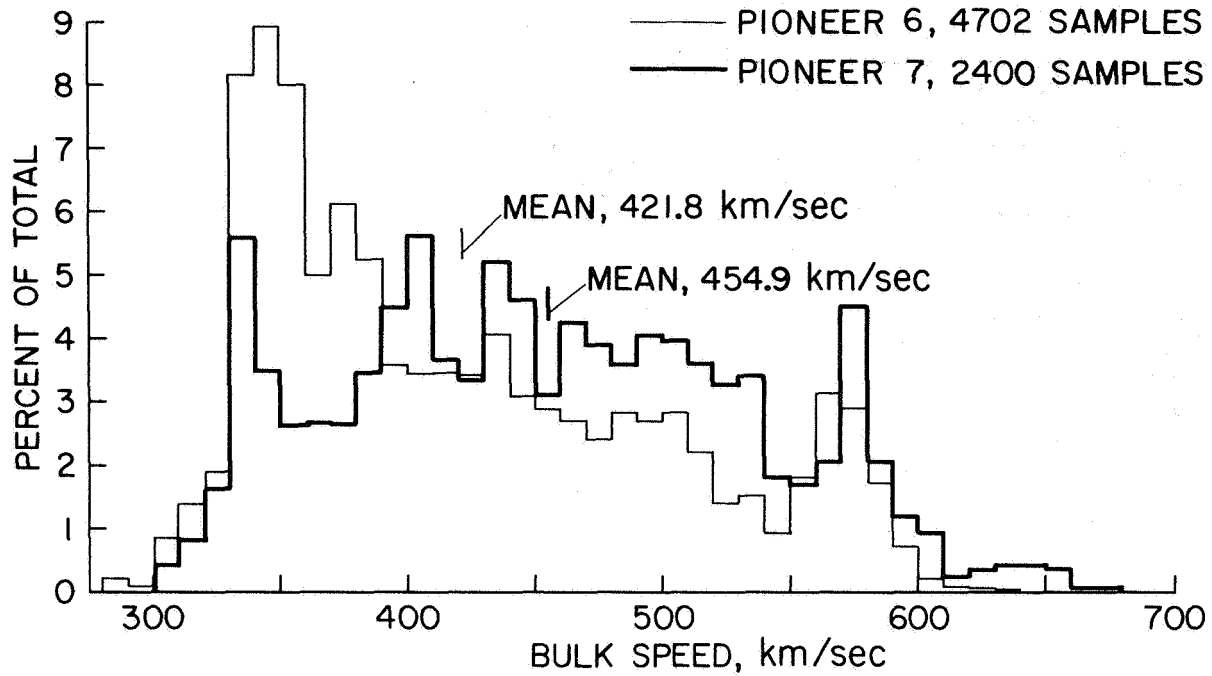Figure 18. *Vela 3 solar wind bulk velocity histogram.*

180

Figure 19. *Pioneer 6 and Pioneer 7 solar wind bulk velocity histogram.*
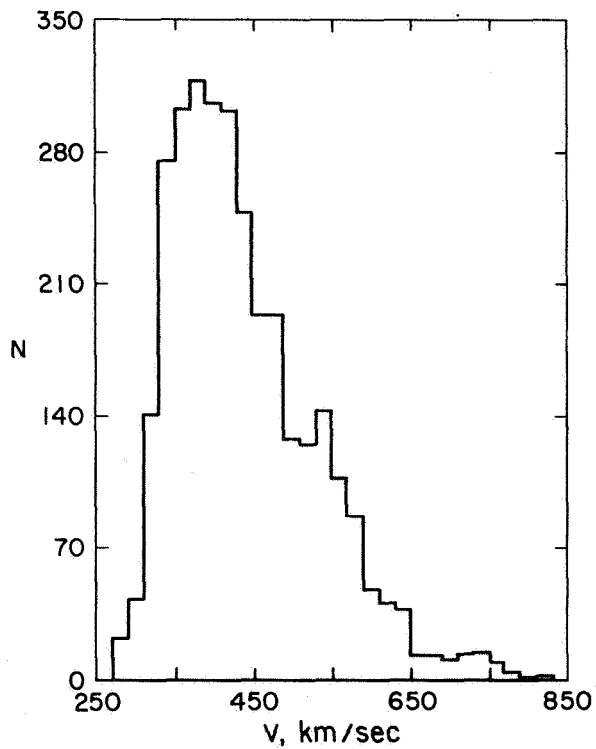

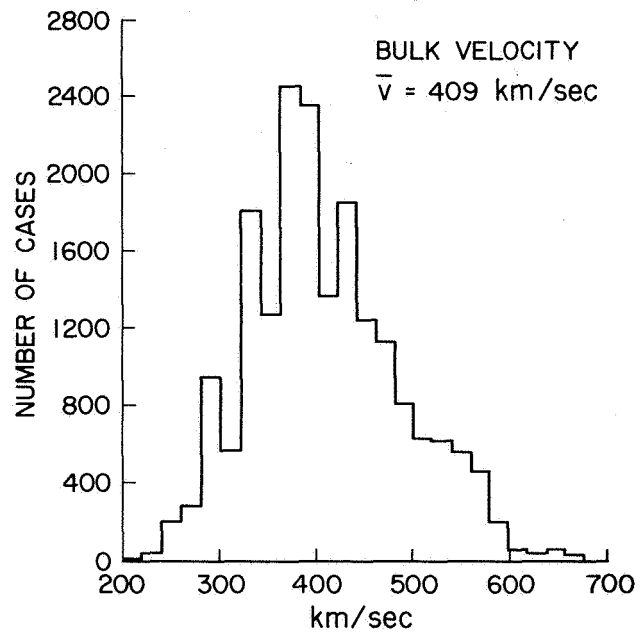**Figure 20.** *Explorer 34 solar wind bulk velocity histogram.*

Figure 21. *HEOS 1 solar wind bulk velocity histogram.*

181

over the period from June to December 1967. The velocities given are 3-hr averages included in 20 km/sec velocity intervals. Here the most probable velocity was approximately 390 km/sec and the average velocity was 438 km/sec. The last velocity histogram (fig. 21), was obtained from HEOS 1 [*Egidi et al.*, 1970] from 2100 hours of observations in the period from December 1968 to April 1969 and from August 1969 to January 1970. Individual cases are shown in 20 km/sec velocity intervals. For the HEOS 1 results, the most probable velocity was 390 km/sec and the average velocity was 409 km/sec.

The most common feature among the various velocity histograms is the skew in the distributions out to a high velocity tail. This high velocity skewing evidently indicates that, in general, the solar wind exists in the more quiescent state between streams than at the high velocities associated with the peak of the streams themselves. Another contributing factor is the frequent observation of a much more gradual slope for the negative gradient of velocity associated with the trailing edge of the high velocity stream as compared to the steep slope at the leading edge. Comparison of the results of Pioneer 6 and Pioneer 7 in figure 19, for example, shows that the skew is much more pronounced for Pioneer 6. Although the statistics are not as good for the Pioneer 7 data, the detailed parameters (fig. 12) reveal a much higher frequency of streams during the observations of Pioneer 7 than that observed during the time of Pioneer 6 (see fig. 11).

Similar plots of the frequency distributions of the solar wind proton number density from five separate spacecraft observations are given in figures 22 through 25.
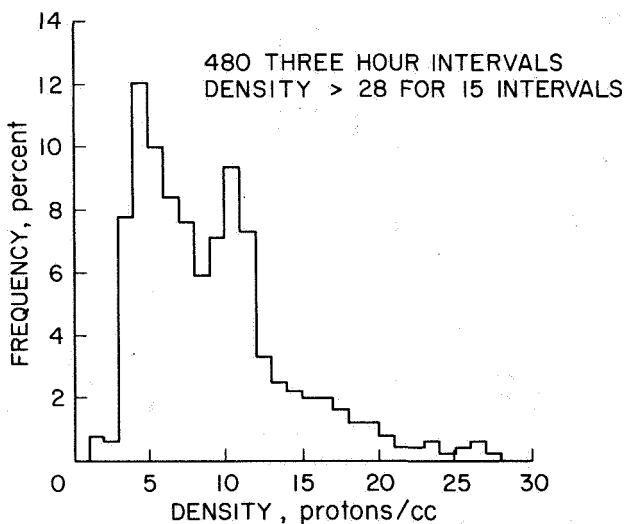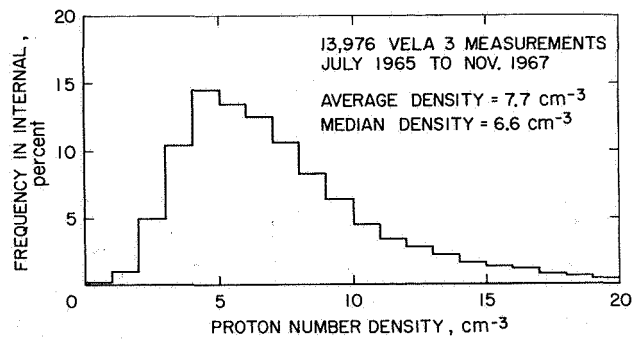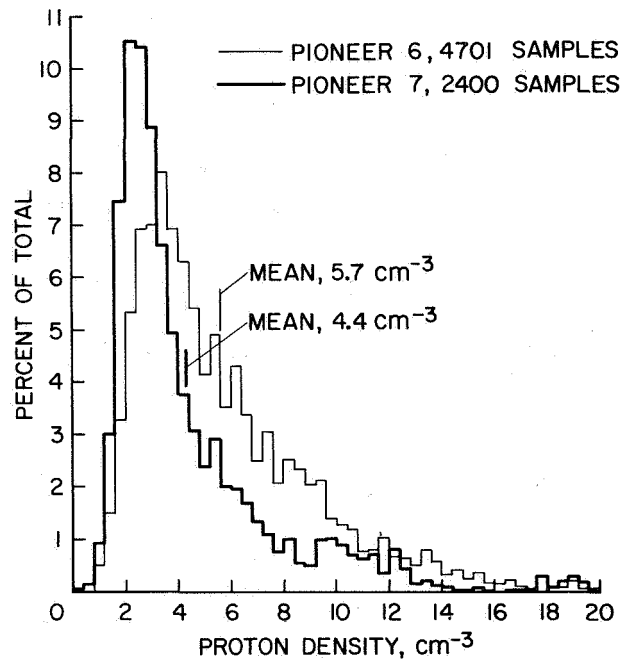

Figure 23. *Vela 3 proton density histogram.*

Figure 24. *Pioneer 6 and Pioneer 7 proton density histogram.*

The density histogram shown in figure 22 was obtained from IMP 1 observations [*Olbert*, 1968] from December 1963 to February 1964. The results shown are 3-hr average values of the density in 1 proton/cm^3 density intervals. For these data the most probable density was approximately 4 cm^{-3} and the average density was 7 cm^{-3}. Figure 23 gives the density histogram from the Vela 3 measurements [*Hundhausen et al.*, 1970]. Individual cases were used with a density interval of 1 proton/cm^3. Here the most probable density was approximately 4 cm^{-3} and the average density was 7.7 cm^{-3}. The density histograms shown in figure 24 [*Mihalov and Wolfe*, 1971] were obtained from Pioneer 6 from December 1965 to February 1966 and from

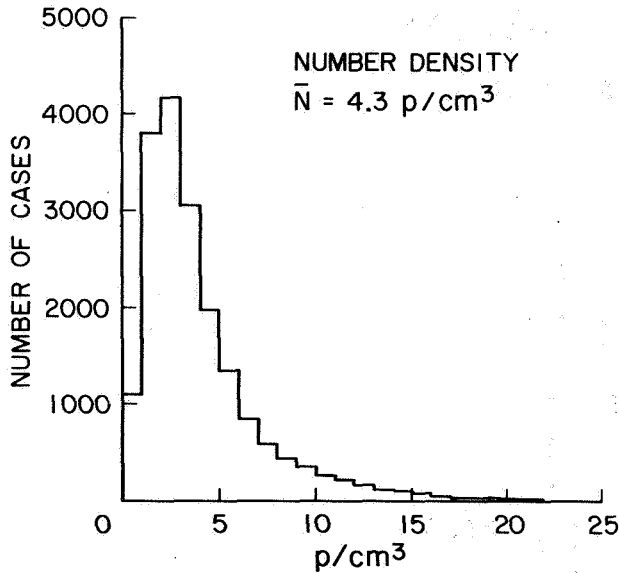Figure 22. *IMP 1 proton density histogram.*

182

Figure 25. *HEOS 1 proton density histogram.*

Pioneer 7 from August to October 1966. Individual cases were used here with a density interval of 0.4 proton/cm^3. The most probable densities for the Pioneer 6 and Pioneer 7 observations were 3.2 and 2.4 cm^{-3}, respectively. The corresponding average densities were 5.7 and 4.4 cm^{-3}. The last density histogram, shown in figure 25, was obtained from the HEOS 1 observations [Egidi et al., 1970] over two time intervals from December 1968 to April 1969 and from August 1969 to January 1970. Individual cases are used and the density interval was 1 proton/cm^3. From the HEOS 1 results the most probable density was approximately 2 cm^{-3} and the average density was 4.3 cm^{-3}.

As was the case for velocity, all the density histograms show a high degree of skewing. Note that the distributions of density all show a tail out to 20 cm^{-3} and beyond. The skewing to high values for both the velocity and density might at first be surprising since the velocity and density are expected to be roughly anticorrelated. Careful examination of the data, however, shows that a velocity-density anticorrelation is a gross oversimplification. For example, recalling the Pioneer 6 results shown in figure 11, it is noted that of the 30 days of data presented, only on four of those days did the 24-hr average values of the density exceed approximately 8 cm^{-3}. Assuming December 17-18, 1965, was a positive gradient in velocity, these high density averages were all associated with the density pileup region at the leading edge of the solar wind streams discussed earlier. Figure 11 indicates that most of the time outside the pileup regions the density varies between approximately 3 and

6 cm^{-3} regardless of velocity. The Pioneer 6 density histogram of figure 24 confirms this result.

Of the three convective properties of the solar wind—bulk speed, number density, and flow direction—the latter is the least well understood. This is probably due to the relatively small variations in the flow directions that one observes and the susceptibility of the measurements to systematic error. Historically, the solar wind flow direction has been considered in terms of its azimuthal and polar components in a solar-ecliptic coordinate system. The azimuthal angle is usually defined as the flow component that lies in the ecliptic and is measured with respect to the spacecraft-sun line. This definition of the azimuthal angle is convenient for most spacecraft since it readily allows the subtraction of the aberration of this angle due to the motion of the spacecraft around the sun. The polar angle is measured with respect to the spacecraft-sun line in the orthogonal plane containing the spacecraft, sun, and ecliptic poles. Figures 26 through 28 show the frequency distribution of the azimuthal component of flow from five separate spacecraft observations. For all histograms shown, negative angles represent flow from east of the sun, positive angles for flow from the west and aberration effects have been removed from all the data. For the case of the Vela 2 data shown in figure 26 [Strong et al., 1967] and the Vela 3 data shown in figure 28 [Hundhausen et al., 1970], the azimuthal angle is measured in the spin plane of the spacecraft, which were tilted with respect to the ecliptic on the order of 30°. The Pioneer data shown in figure 27 [Mihalov and Wolfe, 1971] is in the ecliptic, which coincides with the spin plane of all Pioneer spacecraft. The mean azimuthal flow angles from the Vela 2, Pioneer 6, Pioneer 7, Vela 3A, and Vela 3B measurements are -1.4°, +3.0°, +0.31°, -2.52°, and -0.93°, respectively. The +3.0° value
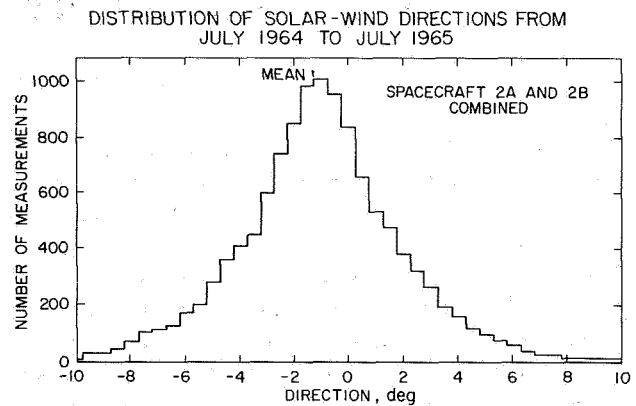

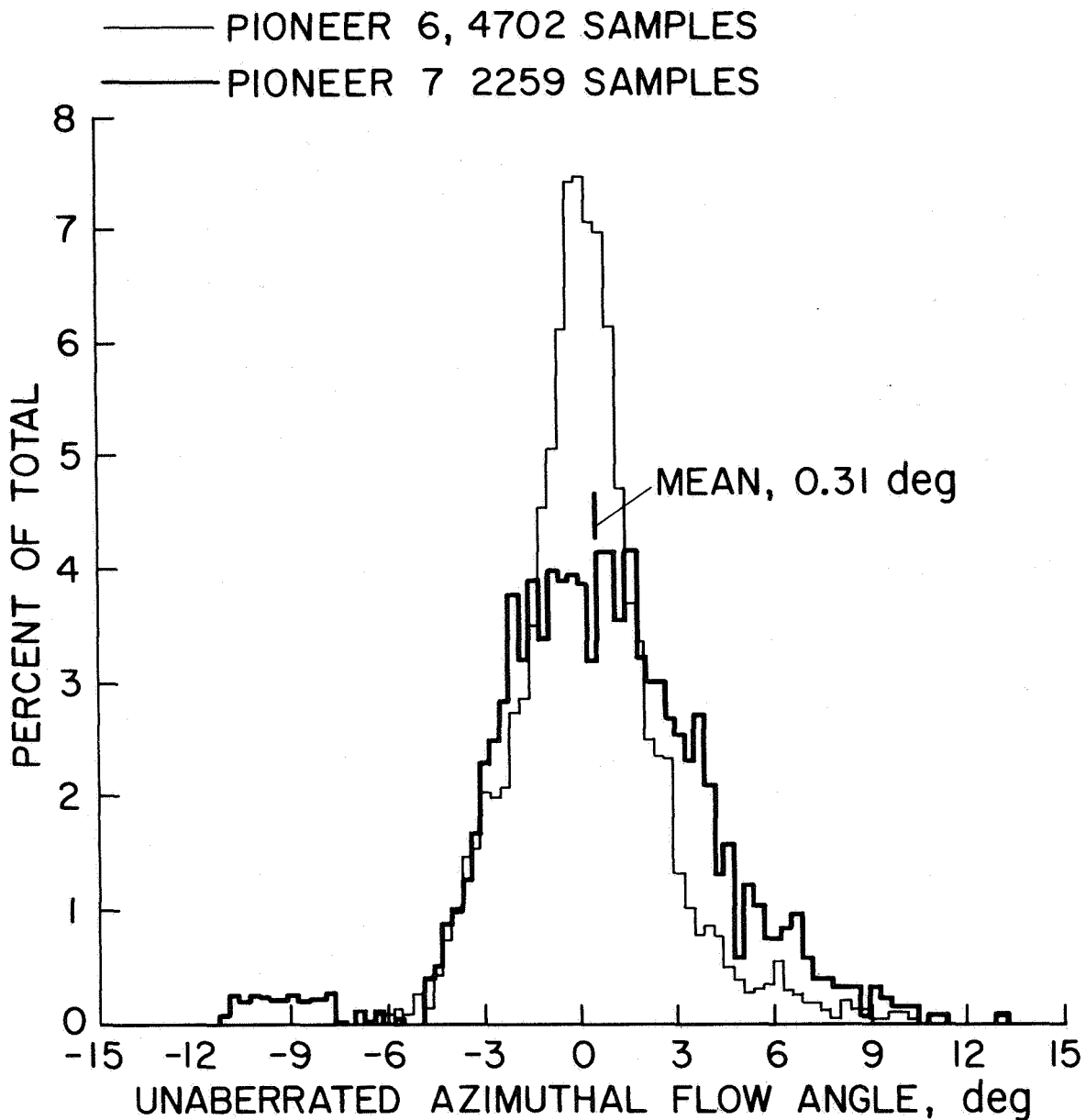**Figure 26.** *Vela 2 solar wind flow direction histogram.*

Figure 27.   *Pioneer 6 and Pioneer 7 azimuthal flow angle histograms.*

obtained from Pioneer 6 was considered a possible systematic error and for comparative purposes was subtracted in the histogram in figure 27. The significant variance in the reported mean values of the azimuthal flow direction leads one to suspect systematic error problems. This is particularly supported by the 1.6° difference in the mean values reported by the Vela 3A and 3B observations, which were taken over the same time interval by presumably identically instrumented spacecraft. Long-term sample aliasing due to noncontinuous observations could also be a contributing factor. In any

event, subtle effects on the solar wind azimuthal flow direction due to solar angular momentum (expected to be only a fraction of a degree) must await more accurate measurements from continuously monitored spacecraft. One of the most interesting features of the azimuthal flow direction distributions is the tendency toward skewing in the direction of flow from west of the sun. Although the azimuthal flow histogram is much more symmetric than the velocity or density distributions, the slight skewing appears to be real. The skewing is particularly evident in the Pioneer and Vela 3 data. Although
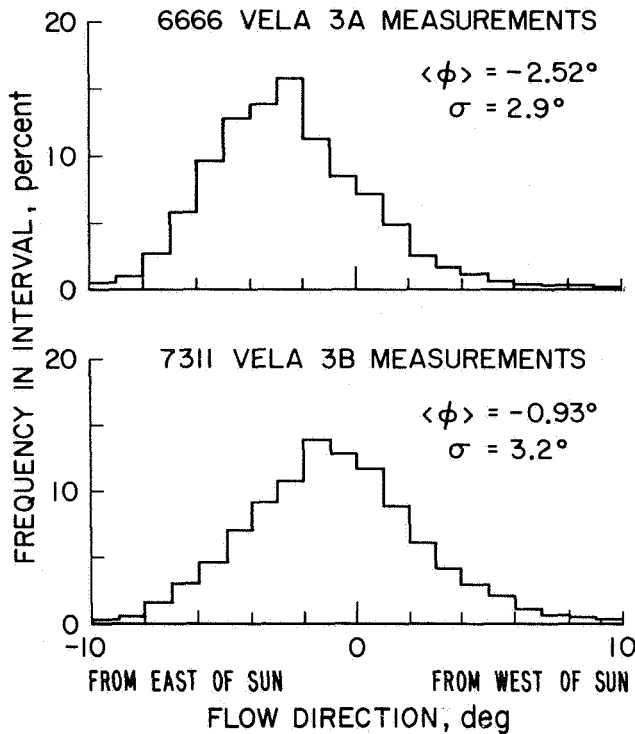
184

Figure 28. *Vela 3A and Vela 3B flow direction histograms.*

Figure 29. *Pioneer 6 and Pioneer 7 polar flow angle histograms.*

conceivably statistical, it is postulated that the skewness is due to the solar wind stream structure. Recalling the stream structure discussed previously, note that the flow from west of the sun, associated with the leading edge of the stream (positive gradient in velocity) was accompanied by high amplitude shifts in the flow direction from west of the sun whereas the negative gradients in velocity, which were associated with azimuthal flow shifts from east of the sun, were of much lower amplitude and much more gradual. This alone seems adequate in accounting for the skewness observed in the azimuthal flow histograms.

Figure 29 shows the distribution in flow direction from the polar component as observed by Pioneer 6 and Pioneer 7 [*Mihalov and Wolfe,* 1971]. The polar flow histograms are the most symmetric of any of the solar wind parameter distributions. The mean values are within experimental error of zero, indicating that the polar component of the solar wind flow is symmetric about the ecliptic. Note that the widths of the polar and azimuthal histograms (fig. 27) are comparable and lead to the conclusion that the stresses on the flow do not have any particular preferred orientations.
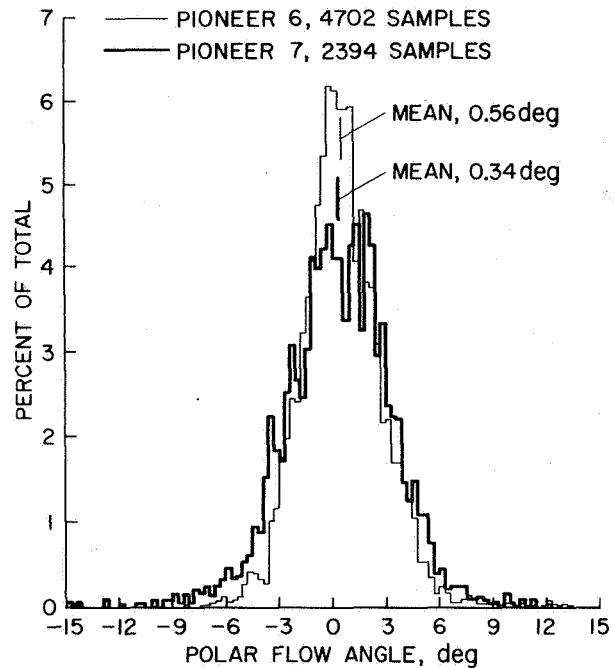
The distributions of the solar wind temperature as observed by six different spacecraft are illustrated in figures 30 through 34. The temperature histogram given in figure 30 was obtained from the Vela 2 results [*Coon,* 1968] from observations made between July 1964 and July 1965. The most probable and mean temperatures are as indicated. Note the skew in the temperature distribution out to approximately 6×10^5 °K. Figure 31
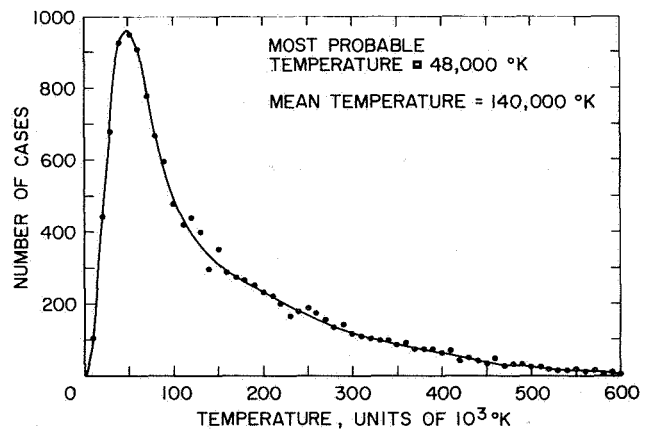

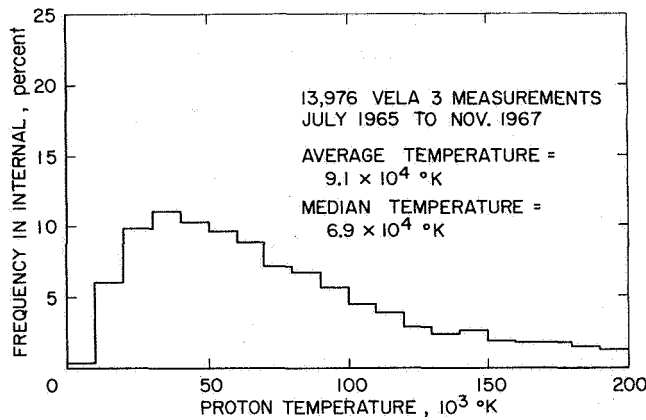Figure 30. *Vela 2 solar wind proton temperature histogram.*
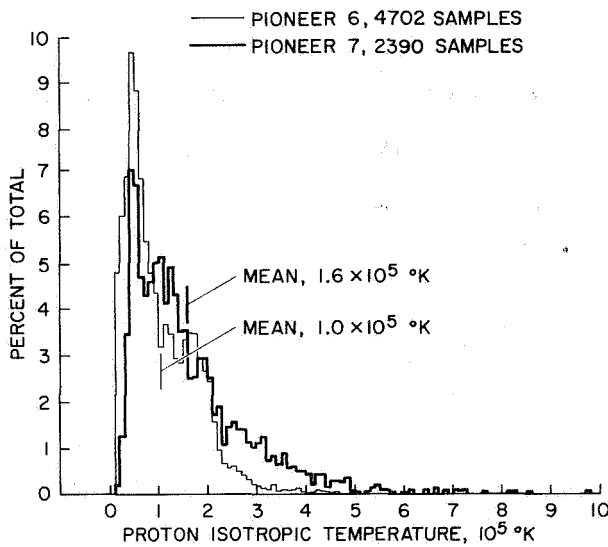
185

Figure 31. *Vela 3 proton temperature histogram.*

13,976 VELA 3 MEASUREMENTS
JULY 1965 TO NOV. 1967

AVERAGE TEMPERATURE =
9.1 × 10⁴ °K
MEDIAN TEMPERATURE =
6.9 × 10⁴ °K

PIONEER 6, 4702 SAMPLES
PIONEER 7, 2390 SAMPLES

MEAN, 1.6 ×10⁵ °K
MEAN, 1.0 ×10⁵ °K

Figure 32. *Pioneer 6 and Pioneer 7 proton temperature histograms.*

Figure 33. *Explorer 34 proton temperature histogram.*

THERMAL SPEED
$\overline{W}$ = 33 km/sec
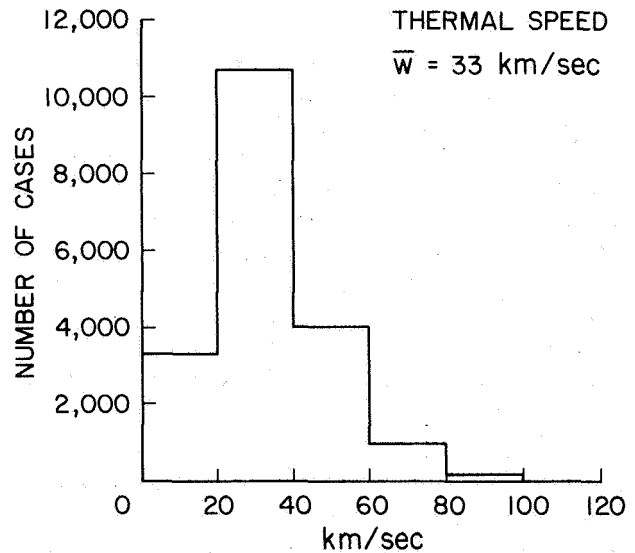
Figure 34. *HEOS 1 proton thermal speed histogram.*

shows the temperature distribution obtained from Vela 3 measurements [*Hundhausen et al.*, 1970] from July 1965 to November 1967. The histogram is plotted out to 2×10^5 °K with 9 percent of the measured values greater than this temperature. The most probable temperature here is approximately 4×10^4 °K and the average temperature is 9.1×10^4 °K. Measurements obtained from Pioneer 6 from December 1965 to February 1966 and Pioneer 7 from August and September 1966 yielded the temperature histograms shown in figure 32 [*Mihalov and Wolfe*, 1971]. The mean temperatures for the two spacecraft are as indicated. The most probable temperatures for Pioneer 6 and Pioneer 7 were 0.4×10^5 °K and 0.3×10^5 °K, respectively. Note the tendency for greater skewing toward higher temperatures for the Pioneer 7
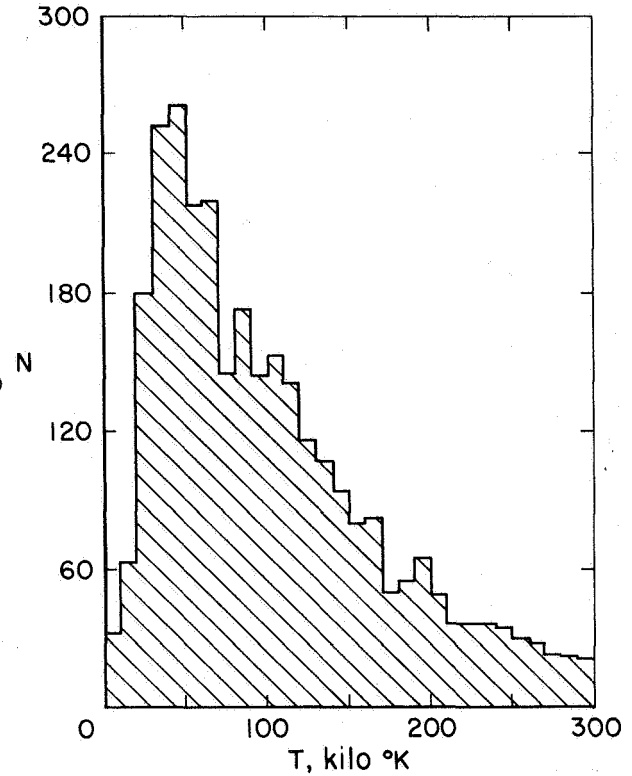
results as compared to Pioneer 6. This evidently reflects the more highly disturbed character of the interplanetary medium and more complex solar wind stream structure at the time of the Pioneer 7 measurements.

Figure 33 shows the temperature distribution obtained from Explorer 34 measurements [*Burlaga and Ogilvie*, 1970] taken from June to December 1967. The most probable temperature was approximately $4.6 \times 10^{4}\,°K$. The average temperature was not reported but is estimated here to be near $10^{5}\,°K$. The temperature distribution obtained from HEOS 1 measurements [*Egidi et al.*, 1970] is shown in figure 34. These results were obtained from 2100 hr of observations during two time intervals from December 1968 to April 1969 and from August 1969 to January 1970. The average temperature is about $6.6 \times 10^{4}\,°K$ where the temperature T is related to the thermal speed W, by $W = (2kT/m)^{1/2}$. The most probable temperature is estimated here to be about $5.5 \times 10^{4}\,°K$.

The most common feature of all of the temperature histograms is the large skewing in the distribution forming a long, high temperature tail. The temperature distributions are generally the most skewed of any solar wind parameter. It is interesting to note that although the average temperature varies by almost a factor of 3 among the various observations, the most probable temperatures are all comparable, near $4\text{-}6 \times 10^{4}\,°K$. The above might be explained by differing degrees of complexity in the solar wind stream structure that were present during the various observations. A complex stream structure tends to elevate the high temperature tail leading to a higher average temperature. On the other hand, the solar wind resides a greater percentage of the time in the "between stream" state where the temperatures are lower and comparable regardless of the period of observation.

With the exception of the Vela 3 results, all the temperature histograms shown are plotted in terms of an isotropic temperature. The Vela 3 histogram is plotted using an effective temperature and will be discussed later. An isotropic temperature assumes that the random motions of the protons obey an isotropic maxwellian distribution law. Although valid to a first approximation, this assumption is not strictly true, as illustrated in figure 35 [*Hundhausen et al.*, 1967], which shows contours of constant flux in a plane in velocity space from Vela 3B in August 1965. The contours are plotted in 10 percent increments decreasing outward from the maximum central contour. The abscissa is the velocity radially outward from the sun and the ordinate is the perpendicular velocity in the spin plane of the Vela 3B satellite. At the time of these measurements, the spin plane was tilted approximately $35°$ with respect to the ecliptic. The arrow represents the orientation of the interplanetary magnetic field projected onto the coordinate plane. The magnetic field orientation was determined by the Goddard Space Flight Center

magnetometer on IMP 3 for the period of the Vela 3B measurements. The triangle near the center of the distribution represents the bulk velocity, which for this case was 347 km/sec in the radial direction and 20 km/sec in the orthogonal direction. The distribution around the bulk velocity is due to the random motions of the protons, and deviations from a circular pattern centered above the bulk velocity are a result of anisotropy. The particular distribution shown in figure 35 is highly anisotropic with an elongated tail symmetric about the magnetic field projection and outward away from the sun.
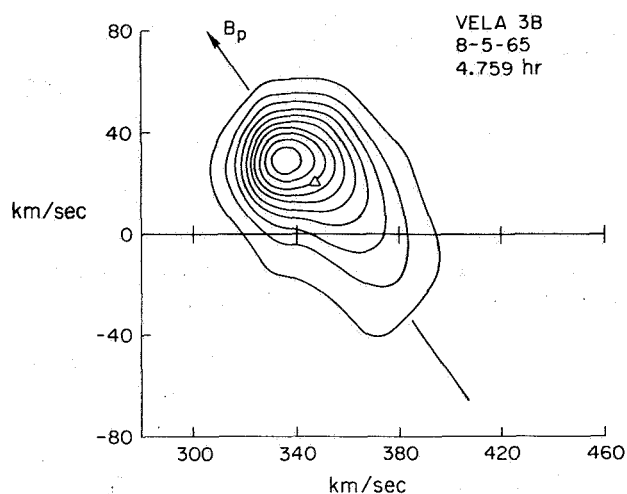
Figure 35. *A contour mapping in the Vela 3 spin plane of an example proton velocity distribution function. The small triangle indicates the mean velocity. The B_p indicates the magnetic field orientation of the time of the measurements.*

Assuming the random motion in the distribution shown in figure 35 to be thermal, *Hundhausen et al.*, [1967] derived the polar plot of temperature given in figure 36. The coordinates and magnetic field are as before. For this case, the maximum temperature seems to be near $120°$ and is approximately $9.2 \times 10^{4}\,°K$. The minimum temperatures lie near the $30°$ and $210°$ radial lines. Defining the anisotropy as the ratio of the maximum to minimum temperatures gives, for this case, a value of about 3.4. Comparison of Vela 3 and IMP 3 data at other times seems to confirm that the anisotropy is, in general, alined with the magnetic field but that the elongated tail is always outward from the sun regardless of the polarity of the field. This elongated tail in the temperature distribution outward from the sun was interpreted as an energy transport or heat conduction away from the sun and estimated to be on the order of 10^{-5} ergs cm^{-2} sec^{-1}. This proton heat conduction is
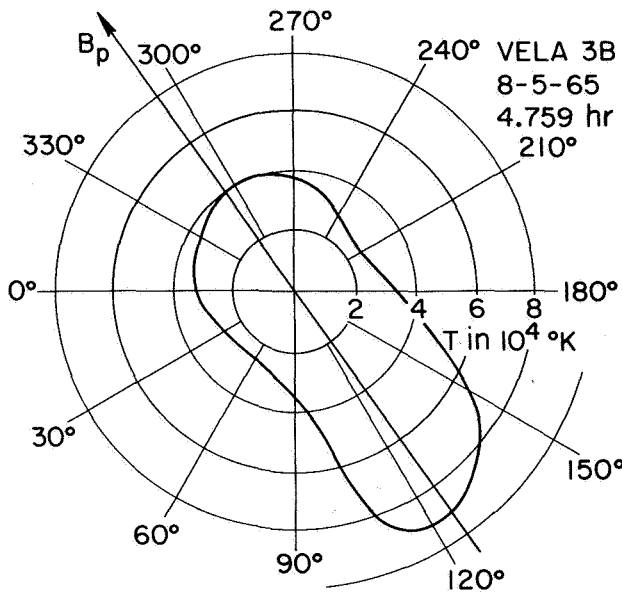
Figure 36. *A polar graph of the temperature for the proton distribution function of figure 35.*

small, however, compared to the electron heat conduction [*Montgomery et al.*, 1968], which is about three orders of magnitude larger.

The anisotropy value of 3.4 for the case discussed above is unusually high as shown in figure 37 [*Hundhausen et al.*, 1970]. This histogram was obtained from the Vela 3 measurements over the time period from July 1965 to November 1967. The most probable value of the anisotropy is between 1.2 and 1.3 and the average value is about 1.9. Note that only 9.6 percent of the determined anisotropy values are greater than 3.0. The anisotropy arises from simple conservation of the magnetic moment of the proton as the collisionless solar wind flows outward from the sun. Theoretical calculations, however, typically predict anisotropy values generally one to two orders of magnitude greater than those
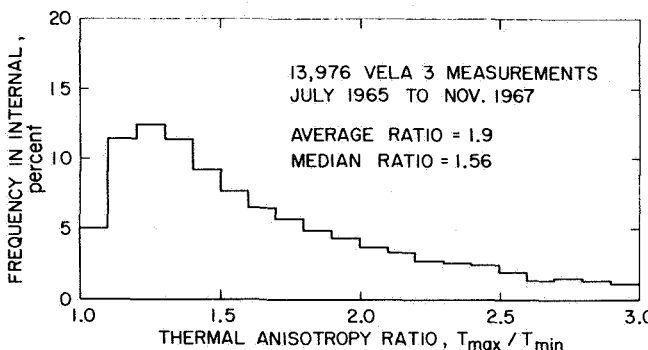
observed. This clearly indicates that instabilities and wave-particle interactions must play an important role in inhibiting the growth of the anisotropy to such high values.

SOLAR WIND PARAMETER RELATIONSHIPS

Up to the present, only the temporal behavior and variance or frequency distribution of the individual solar wind parameters have been dealt with. Consider now a more detailed investigation of the relationships between various solar wind parameters. Figure 38 shows the solar wind proton density as a function of flow speed from measurements made by the Vela 3 satellites [*Hundhausen et al.*, 1970] during the period from July 1965 to November 1967. The density is plotted as the average within a 25 km/sec flow speed interval. For
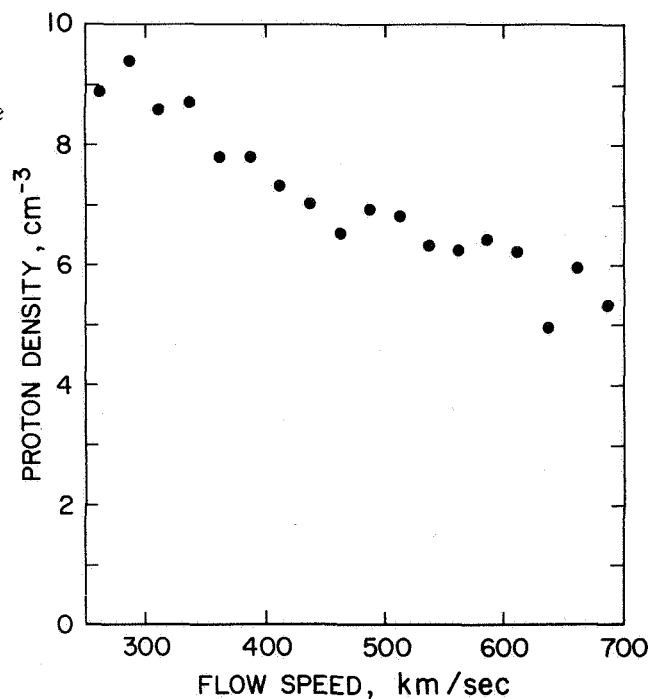

Figure 38. *Vela 3 proton density versus solar wind flow speed.*

these observations the density is observed to decrease with increasing velocity almost as V^{-1} (constant flux) up to about 500 km/sec, beyond which the density tends to level off. The relationship between density and velocity observed by the Ames Research Center plasma probe on Pioneer 6 from December 1965 to March 1966 is shown in figure 39. Here the results are presented somewhat differently than in the previous figure with each point representing a 24-hr average value of the proton density and velocity. These results suggest a

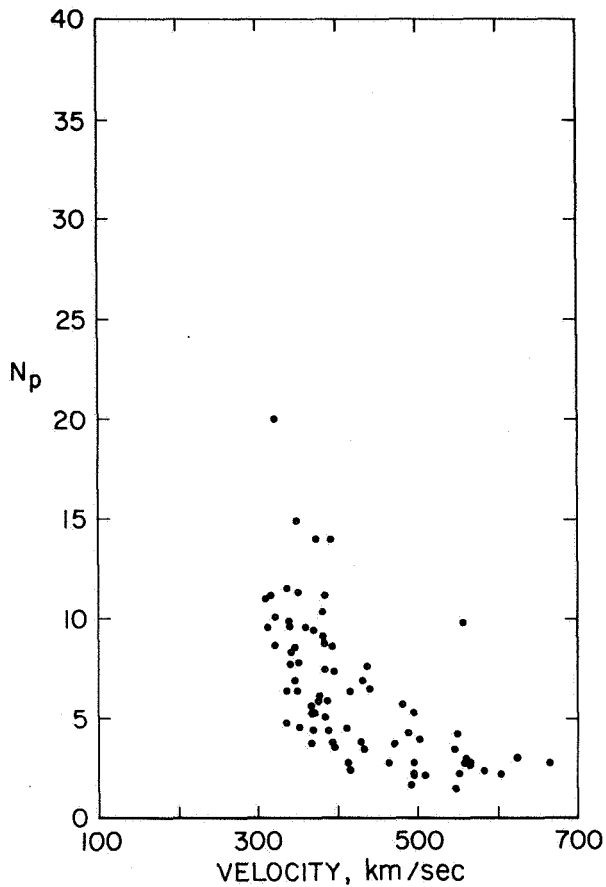**Figure 37.** *Vela 3 thermal anisotropy histogram.*

Figure 39. *Pioneer 6 proton number density versus velocity.*

Figure 40. *Explorer 34 proton number density versus velocity. Average values from other spacecraft are shown in the circles.*

much more exponential fall off of density with increasing velocity, particularly at the lower velocities. Note the large scatter in the density for low velocities. This can be accounted for by recalling that densities in the range of about 4 to 7 cm^{-3} are typical of the solar wind in the "between stream" state where the velocity is low. On the other hand, densities greater than 7 cm^{-3} are more typical of the "pileup" regions ahead of new streams where the velocity is also relatively low. The exponential character of the density-velocity relationship clearly indicates why the density and velocity frequency distributions both tend to peak at low values with skewing toward the higher values of both parameters. The density-velocity relationship obtained by Explorer 34 [*Burlaga and Ogilvie*, 1970b] and some average values obtained from several other spacecraft observations are given in figure 40. The Explorer 34 observations cover
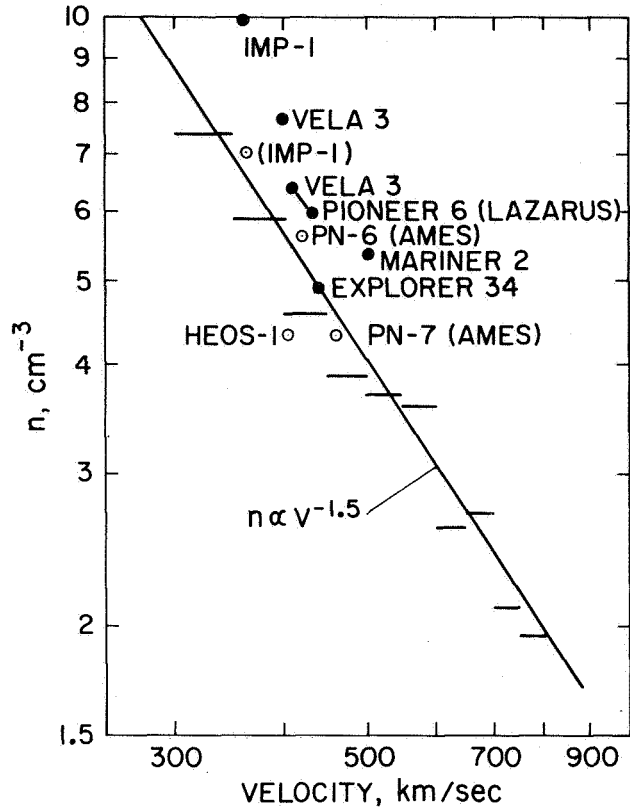
the period from June to December 1967 and the horizontal lines represent the average density within 50 km/sec velocity intervals. The individual points represent the average values of density and velocity for the various spacecraft observations indicated. The open points are further observations that have been added to the original figure of *Burlaga and Ogilvie* [1970b]. The lower density IMP 1 average is a corrected value [*Olbert*, 1968] and the higher density IMP 1 point should be ignored. The best-fit curve to the Explorer 34 results indicates a density dependence on velocity of $V^{-1.5}$. Although the various observations show some scatter, it is clear that density decreases exponentially with velocity and that on the average the solar wind flux is not a constant. The above must be accounted for by any theory that attempts to determine the solar wind source function.

Consider next the relationship between the solar wind flow direction and velocity. Figure 41 [*Hundhausen et al.*, 1970] gives the average flow direction in the Vela 3A and 3B spin planes as a function of the flow speed in 25 km/sec intervals. The results were obtained from measurements made during the interval from July 1965
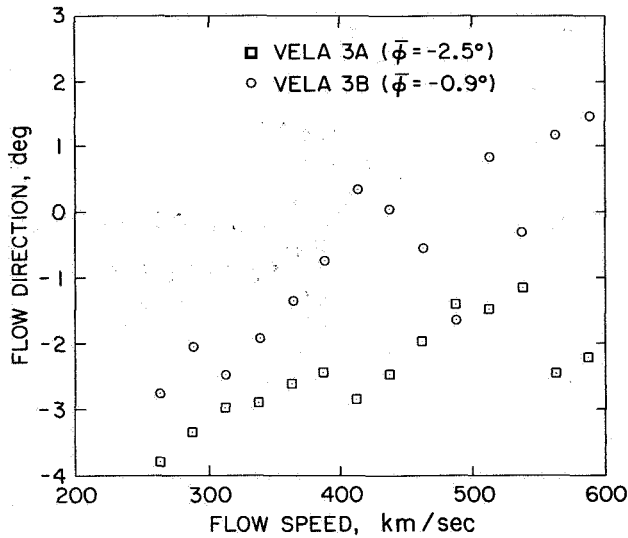
**Figure 41.** *Vela 3A and Vela 3B flow directions versus flow speed.*

to November 1967. Since the Vela 3 spin planes are tilted approximately 35° with respect to the ecliptic, then in a solar-ecliptic coordinate system, the flow directions given here contain contributions from both the azimuthal and polar components. Wolfe [1970], however, has shown from Pioneer 6 results that there is no discernible correlation between the polar component and the flow speed; therefore the results shown here presumably reflect only contributions from the azimuthal component. Due to the likelihood of systematic error and for comparative purposes, the obvious trend toward more positive flow with increasing velocity should be considered the important feature of the flow direction-velocity relationship rather than the absolute values. Note in the Vela 3A data the tendency for the return of the flow toward the negative direction at the highest velocities. Although conceivably statistical, this trend is also seen in the Pioneer 6 results [Wolfe, 1970] given in figure 42. Plotted here are 3-hr average values of the azimuthal flow direction and corresponding velocity from measurements made over one complete solar rotation beginning December 18, 1965. The average azimuthal flow direction for this entire time interval was +2.6° (flow from west of the sun). This average is considered to be possibly a systematic error and has been arbitrarily subtracted from all the data to permit investigation of trends in the azimuthal flow direction with respect to a zero mean. The trend toward more positive flow with increasing velocity is also readily seen in the Pioneer 6 results; however, the return to more nearly radial flow at the higher velocities is quite pronounced.
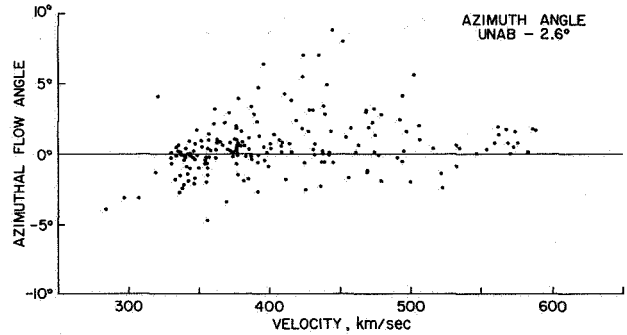
Figure 42. *Pioneer 6 3-hr average values of the azimuthal flow angle as a function of velocity.*

Note also the large scatter in azimuthal angles most prominent between about 400 and 450 km/sec. Recalling the more detailed data discussed in connection with the solar wind stream structure, the largest amplitude variations in the azimuthal flow direction (particularly positive) were associated with the leading edge (sharp positive velocity gradient) of a new stream where the velocity was typically on the order of 400-450 km/sec. Recall also that near the peak of the stream (highest velocity) the flow tended to be more radial. Thus, the correspondence between the azimuthal flow direction and velocity seen here seems clearly to be highly dependent on the solar wind stream structure.

Figure 43 [Wolfe, 1970] shows the relationship between the polar and azimuthal flow directions
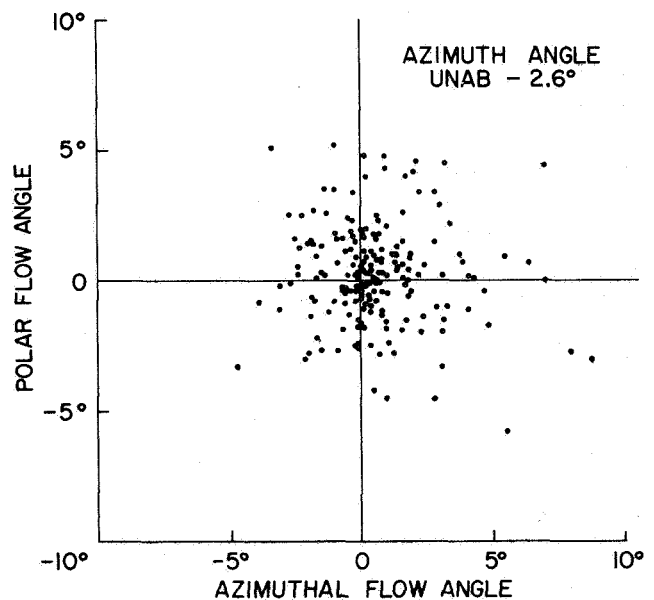
Figure 43. *Pioneer 6 polar flow angle as a function of azimuthal flow angle.*

obtained from Pioneer 6 over the same time interval as the previous figure. As before, the azimuthal angles have been corrected by 2.6° for comparative purposes. By inspection it is seen that the polar and azimuthal flow components are completely independent. It is interesting to note, however, that the amplitude in the flow angle variations are comparable for the two components.

The relationship between temperature and velocity is very strong, as indicated by the Vela 3 results shown in figure 44 [*Hundhausen et al.*, 1970]. These results were compiled from observations made from July 1965 to November 1967. The temperatures are averages in 25 km/sec flow speed intervals. A similar strong temperature-velocity relationship is also indicated by Ames Research Center plasma observations from Pioneer 6 during the period December 1965 to March 1966 (fig. 45). The values given are 24-hr averages with the temperature plotted on a logarithmic scale. For reference purposes the square root of T relationship with velocity determined by *Burlaga and Ogilvie* [1970a] derived from Explorer 34 observations is also plotted on the Pioneer 6 data. Although the Pioneer 6 results seem to fit this relationship fairly well, there is a great deal of
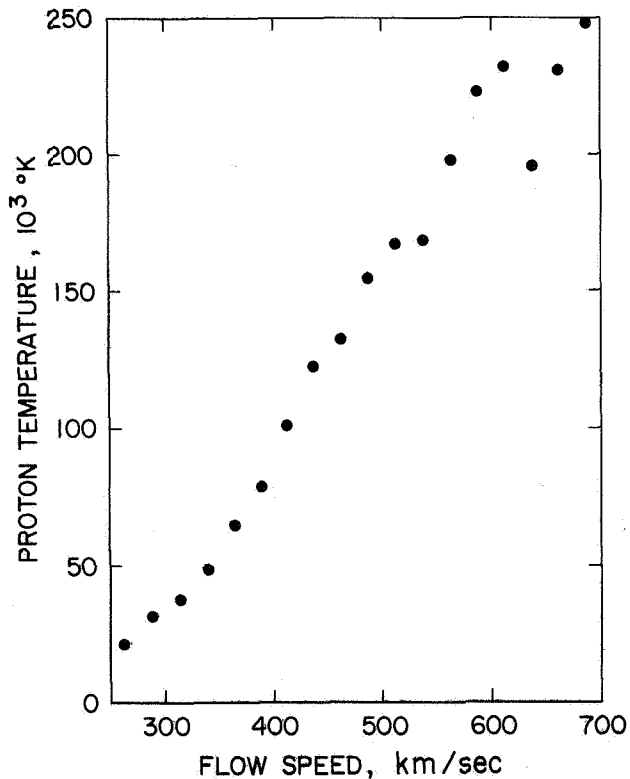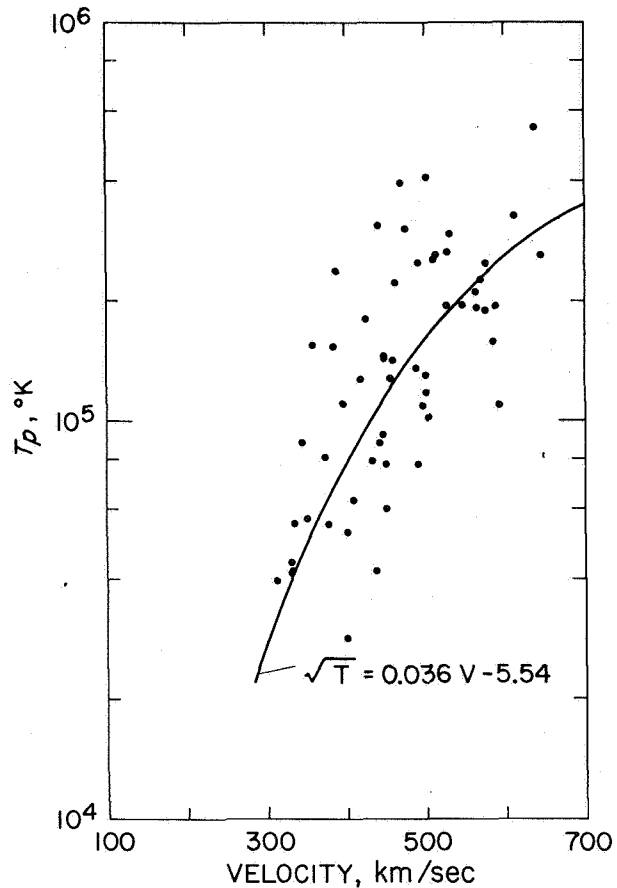

Figure 45. *Pioneer 6 proton temperature versus velocity.*

scatter, and a linear relationship seems to fit about as well. This is also true for the Vela 3 results of figure 44. Note, however, the particularly large amount of scatter (in the direction of higher temperature with respect to the curve) between about 350 and 500 km/sec. This is conceivably due to the heating one observes associated with the positive gradient in velocity on the leading edge of a solar wind stream where the velocities are typically in this range. Figure 46 shows the relationship between the anisotropy, defined by T_{max}/T_{min} [*Hundhausen et al.*, 1970], and the flow speed. These results were obtained from Vela 3 measurements over the period from July 1965 to November 1967 with the anisotropy averaged in 50 km/sec flow speed intervals. The average anisotropy is seen to peak near 375 km/sec at a value of approximately 2.0, and to drop off slightly for lower velocities and much more steeply for higher velocities. *Hundhausen et al.* [1970] postulated the fall off of anisotropy for the low velocities as consistent with coulomb collision effects and the decrease in anisotropy
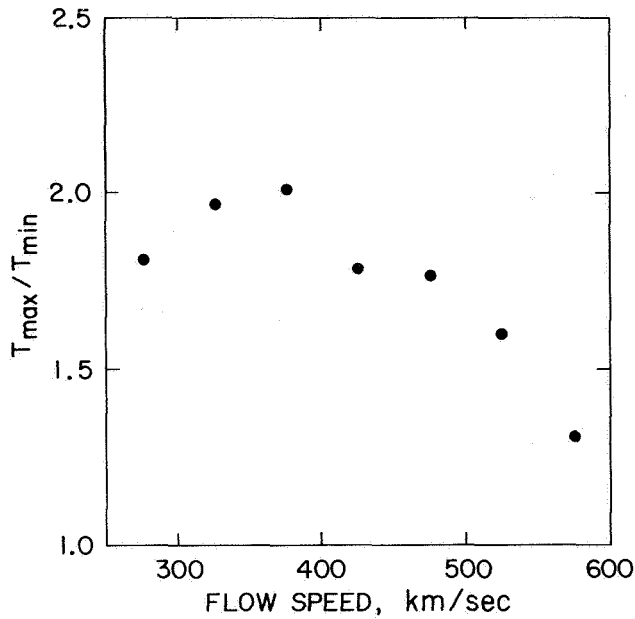

Figure 44. *Vela 3 proton temperature versus flow speed.*

Figure 46. *Vela 3 anisotropy versus flow speed.*

Figure 47. *Mariner 2 scatter diagram of daily mean plasma velocity versus* ΣK_p. *The line is the least squares linear fit to the points.*

Figure 48. *IMP 1 daily averages of the solar wind velocity plotted versus the daily sum of the* K_p *index.*

with increasing velocity above 375 km/sec to be the result of the dominance of instabilities associated with a more disturbed medium.

INTERPLANETARY-TERRESTRIAL RELATIONSHIPS

The interplanetary-terrestrial relationship that has been sought historically is that between the character of the solar wind and the state of the geomagnetic field. *Snyder et al.* [1963] made the first attempt to establish this relationship on the basis of Mariner 2 observations. Of all the solar wind parameters or combinations thereof, the best correlated parameter with the geomagnetic disturbance index K_p was the solar wind flow speed. These results are shown in figure 47 where the 24-hr average velocity is plotted against the daily sum of K_p for that particular day. The results were obtained during the period from late August through late December 1962. The line through the data represents the least-squares linear fit to the points. Although the trend of increasing K_p with increasing velocity is certainly evident, the large amount of scatter in the data obscures a possibly, strong relationship between velocity and K_p. Similar results were reported by *Olbert* [1968] from the MIT IMP 1 observations obtained from November 1963 to February 1964 shown in figure 48. The relationship (assumed linear) between velocity and K_p is somewhat different than the Mariner 2 results, and a large residual scatter remains in the data. The correlation coefficient for these results was approximately 0.8. Figure 49 indicates the

relationship between the 24-hr average solar wind velocities obtained by Pioneer 6 [*Wolfe*, 1970] and the daily geomagnetic disturbance index A_p. The correlation coefficient here is approximately 0.7, and as was the case with the Mariner 2 and the IMP 1 results there is again a large scatter in the data. Perhaps the best explanation of the scatter is the frequently observed phase lag between the solar wind velocity and geomagnetic disturbance indices discussed earlier. During the rising portion or

192

Figure 49. *Pioneer 6 24-hr average values of solar wind velocity versus the A_p index.*

leading edge of a solar wind stream (positive gradient in velocity), the geomagnetic field tends to be much more disturbed than during the trailing portion (more gradual negative gradient) of the stream. Thus for a given value of solar wind velocity the K_p or A_p index would be double valued leading to the scatter observed in figures 47 through 49. As discussed earlier, the de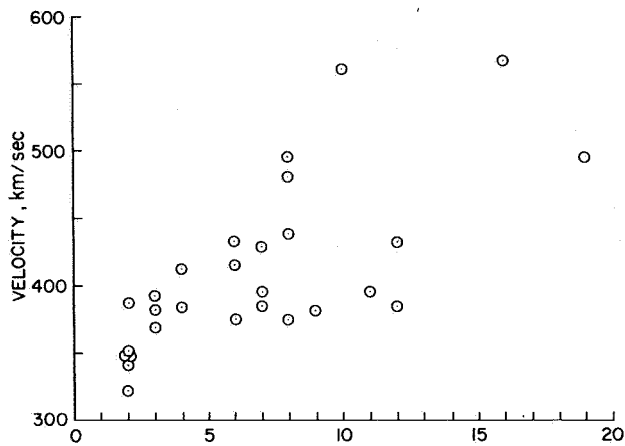nsity tends to lead the velocity lag, and the temperature is approximately in phase with the daily geomagnetic disturbance index A_p (or $\Sigma \ K_p$). Figure 50 gives the 24-hr average values of the Ames Research Center Pioneer 6 solar wind proton temperature observations as a function of the A_p index. These measurements were obtained over the same period as the previous figure. Even though the correlation coefficient here is approximately 0.9, there is still significant scatter in the data. It is inconceivable that the amplitude of the random motion in the protons should really have any strong effect on the geomagnetic field.
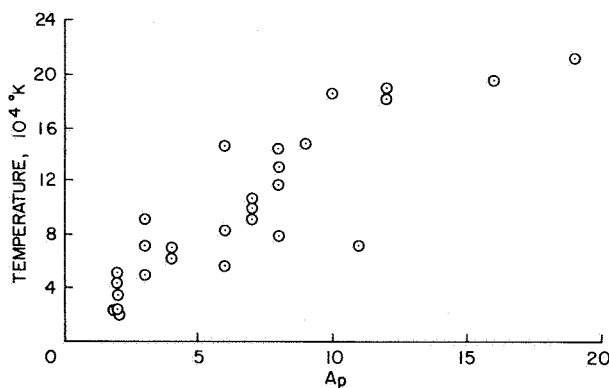

Figure 50. *Pioneer 6 24-hr average values of proton temperature versus the A_p index.*

What seems more plausible is that the solar wind proton temperature represents a large-scale indication of the degree of disturbance in the interplanetary medium, and that changes in the momentum flux or simply flux fluctuations are conceivably responsible for geomagnetic disturbance. The above, however, can only be confirmed by higher time resolution plasma measurements than are presently available. The result that solar wind proton temperature seems to give the best correlation with geomagnetic disturbance indices is considered here to be an effect, not a cause.

EFFECTS OF SOLAR LATITUDE AND RADIAL DISTANCE

Unfortunately, space observations to date have been restricted to near the plane of the ecliptic between the orbits of Venus and Mars. In a spherical coronal expansion model, the solar wind density is expected to decrease as the square of the distance. This has been tentatively verified by the Mariner 2 results [*Neugebauer and Snyder*, 1966] shown in figure 51. Twenty-seven day averages of the daily averages of proton density, flux, and total momentum flux are plotted versus distance from the sun. The slopes for an inverse square relationship are also shown. Considering the variations observed from one solar rotation to the next, the density here seems to fit the expected inverse square relation remarkably well. The Mariner 2 results showed no radial dependence for either the velocity or temperature. This is not unexpected since the radial dependence for these parameters is conceivably much more subtle. As the
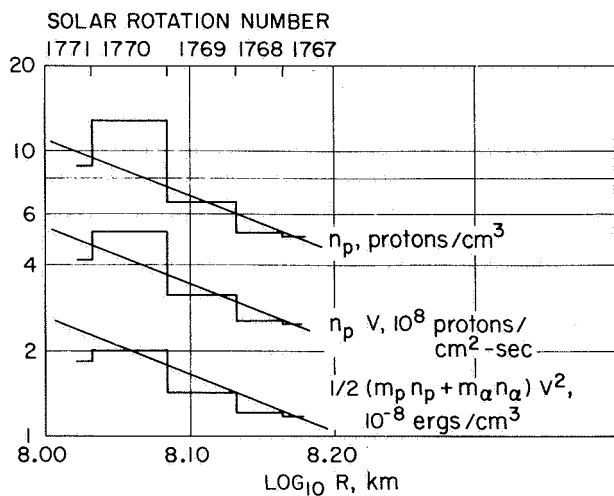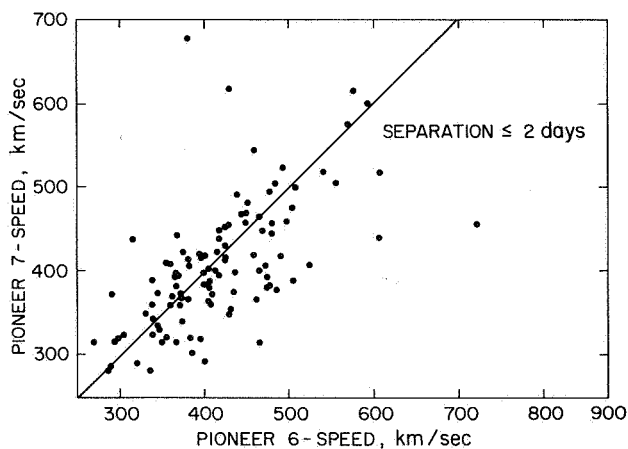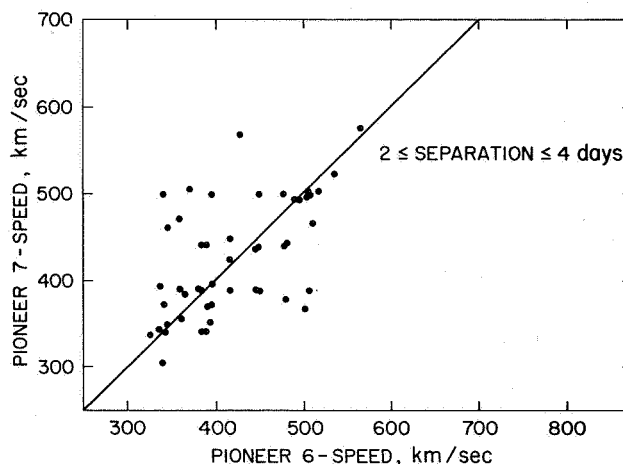

Figure 51. *Mariner 2 27-day averages of the daily averages of proton number density, proton flux and total momentum flux versus distance from the sun. The slopes for an inverse square relation are also given.*

solar wind flows outward from the sun, it is expected to quickly approach a terminal velocity that would be essentially constant beyond the Earth's orbit. The radial variation of the proton temperature is less certain and would be dependent on the proton-heating mechanisms. For example, adiabatic, constant speed expansion with isotropic pressure requires that the proton temperature decrease as $R^{-4/3}$, whereas conduction- dominated flow gives an $R^{-2/7}$ dependence and flow dominated by proton-electron energy exchange has an $R^{-6/7}$ dependence. It seems likely that these dependencies would be difficult to separate from the temporal variations for observations which only extend over a radial distance of approximately 0.3 AU.

Gosling [1971] compared Pioneer 6 and Pioneer 7 velocity observations during the period from January 1969 to July 1970. Specifically, the velocity observed by one spacecraft was compared to the velocity observed by the other spacecraft after a period corresponding to the corotation delay due to their heliocentric azimuthal separation. Figure 52 shows the results when the two spacecraft are separated in corotation by less than two days. With a few exceptions, most of the points tend to lie close to the equal velocity line, although there is some scatter. When the two spacecraft have a separation of 2 to 4 days (fig. 53), the fit is not as good. A separation of greater than 4 days (fig. 54), indicates a very poor correlation. This implies that there are significant coronal changes taking place on a time scale of a few days (at least at the time of these measurements) and predicts the difficulty of determining the solar wind radial gradients from a single spacecraft. However, one cannot discount the possibility that this is a heliographic

Figure 53. *Comparison of Pioneer 7 and Pioneer 6 solar wind flow speeds when the two spacecraft are separated by 2 to 4 days corotation delay.*
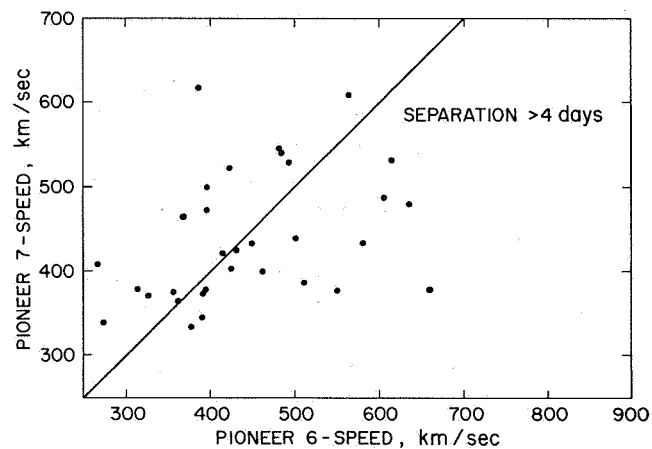
Figure 54. *Comparison of Pioneer 7 and Pioneer 6 solar wind flow speed when the two spacecraft are separated by greater than 4 days corotation delay.*

Figure 52. *Comparison of Pioneer 7 and Pioneer 6 solar wind flow speeds when the two spacecraft are separated by less than 2 days corotation delay.*

latitude effect due to the tilt of approximately 7° of the sun's equatorial plane with respect to the ecliptic.

In considering what might be expected in the way of heliographic latitude effects on the solar wind, a coronagraph photo of the March 7, 1970, solar eclipse is shown in figure 55 [*Smith*, 1970]. This is a composite of three separate pictures with the north pole of the sun at the
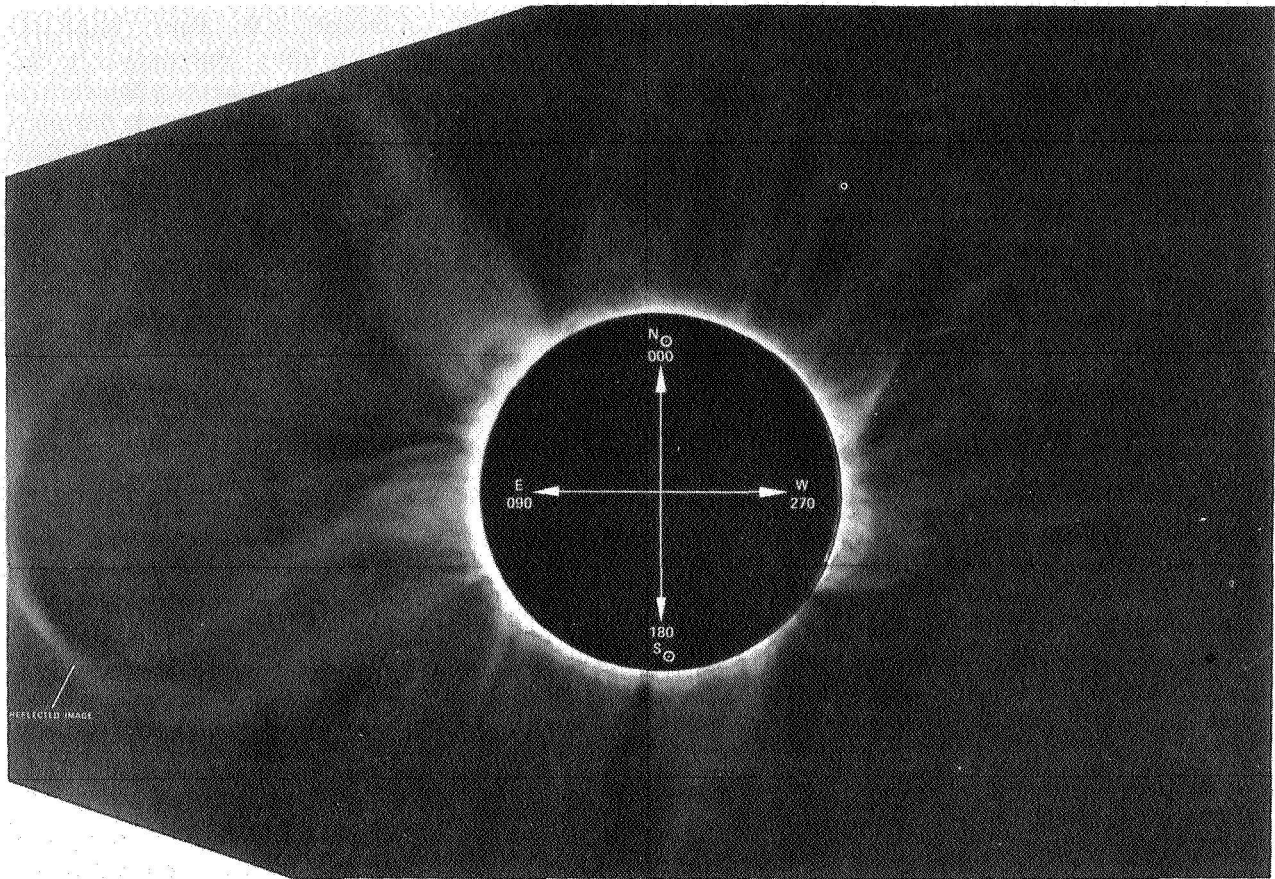
194

Figure 55. *Composite of 3 coronagraph photos of the March 7, 1970 solar eclipse.*

top. Note in particular that the coronal streamers are just as prevalent near the solar pole as they are near the equator. If these streamers play an important role in solar wind dynamics, then one might not expect any significant solar wind latitude effects. However, one might expect drastic effects on the character of the stream interactions since with increasing heliographic latitude the interplanetary magnetic field becomes less and less spiraled. The observation of these effects will probably require space measurements up to at least 30° to 40° heliographic latitude.

REFERENCES

Burlaga, L. F.; and Ogilvie, K. W.: Heating of the Solar Wind. *Ap. J.*, Vol. 159, 1970*a*, pp. 659-670.

Burlaga, L. F.; and Ogilvie, K. W.: Magnetic and Kinetic Pressures in the Solar Wind. *Solar Phys.*, Vol. 15, 1970*b*, pp. 61-71.

Coon, J. H.: Solar Wind Observations, in *Earth's Particles and Fields*. edited by B. M. McCormac, Reinhold, New York, 1968, pp. 359-372.

Egidi, A.; Formisano, V.; Moreno, G.; Palmiotto F.; and Saraceno, P.: Solar Wind and Location of Shock Front and Magnetopause at the 1969 Solar Maximum. *J. Geophys. Res.*, Vol. 75, 1970, pp. 6999-7006.

Gosling, J. T.: Variations in the Solar Wind Speed Along the Earth's Orbit. *Solar Phys.*, 1971 (in press).

Hundhausen, A. J.; Bame, S. J.; and Ness, N. F.: Solar Wind Thermal Anisotropies: Vela 3 and IMP-3. *J. Geophys. Res.*, Vol. 72, 1967, pp. 5265-5274.

Hundhausen, A. J.; Bame, S. J.; Asbridge, J. R.; and Sydoriak, S. J.: Solar Wind Proton Properties: Vela 3 Observations from July 1965 to June 1967. *J. Geophys. Res.*, Vol. 75, 1970, pp. 4643-4657.

Lyon, E.; Egidi, A.; Pizzella, G.; Bridge, H.; Binsack, J.; Baker, R.; and Butler, R.: Plasma Measurements on Explorer 33, (1) Interplanetary Region. *Space Research VIII*, edited by A. P. Mitra, L. G. Jacchia and W. S. Newman, North-Holland Publishing Co., Amsterdam, 1968, pp. 99-106.

Mihalov, J. D.; and Wolfe, J. H.: Average Solar Wind Properties from Pioneers 6 and 7. *Cosmic Electrodynamics,* Vol. 2, 1971, pp. 326- 339.

Montgomery, M. D.; Bame, S. J.; and Hundhausen, A. J.: Solar Wind Electrons: Vela 4 Measurements. *J. Geophys. Res.,* Vol. 73, 1968, pp. 4999-5003.

Neugebauer, M.; and Snyder, C. W.: Mariner 2 Observations of the Solar Wind, 1. Average Properties. *J. Geophys. Res.,* Vol. 71, 1966, pp. 4469-4484.

Olbert, S.: Summary of Experimental Results from MIT Detector on IMP-1. *Physics of the Magnetosphere,* edited by R. L. Carovillano, D. Reidel, Dordrecht-Holland, 1968, pp. 641-659.

Parker, E. N.: Dynamics of the Interplanetary Gas and Magnetic Fields. *Astrophys. J.,* Vol. 128, 1958, p. 664.

Smith, S.: Solar Eclipse 1970. Bulletin F, National Science Foundation, 1970, p. 157.

Snyder, C. W.; Neugebauer, M.; and Rao, U. R.: The Solar Wind Velocity and its Correlation with Cosmic-Ray Variations and with Solar and Geomagnetic Activity. *J. Geophys. Res.,* Vol. 68, 1963, pp. 6361-6370.

Strong, I. B.; Asbridge, J. R.; Bame, S. J.; and Hundhausen, A. J.: Satellite Observations of the General Characteristics and Filamentary Structure of the Solar Wind. *The Zodiacal Light and the Interplanetary Medium,* edited by J. L. Weinberg, National Aeronautics and Space Administration, Washington, D. C., 1967, pp. 365-372.

Wilcox, J. M.; and Ness, N. F.: A Quasi-stationary Co-rotating Structure in the Interplanetary Medium. *J. Geophys. Res.,* Vol. 70, 1965, pp. 5793-5805.

Wilcox, J. M.; and Colburn, D. S.: Interplanetary Sector Structure in the Rising Portion of the Sunspot Cycle. *J. Geophys. Res.,* Vol. 74, 1969, pp. 2388-2392.

Wilcox, J. M.; and Colburn, D. S.: Interplanetary Sector Structure Near the Maximum of the Sunspot Cycle. *J. Geophys. Res.,* Vol. 75, 1970, pp. 6366-6370.

Wolfe, J. H.: Solar Wind Characteristics Associated with Interplanetary Magnetic Field Sector Structure. *Trans. Amer. Geophys. Union,* Vol. 51, 1970, p. 412.

DISCUSSION   *E. R. Schmerling* I have a very naive view of the sun as something that emits the solar wind and has a few small active regions on it. From this view I can see very readily why your curves of velocity and temperature should be skewed towards the high end. If you follow up you can understand why your curves of density are also skewed along the high end. However, you stated that there are inverse relationships between density and velocity and between density and temperature. Would you explain?

J. H. Wolfe The skew toward the high end for the density comes primarily from the pileup region near the leading edge of a new stream. The solar wind velocity is fairly low there. The density structure is maybe two or three days wide, whereas the velocity structure is many days wide. Overall the density seems to be "anticorrelated."

R. H. Dicke For the solar wind torque calculations one would like the product of the density by the velocity. Is there information about the way the mean values of this product vary through the sunspot cycle?

J. H. Wolfe I tried to point out that there doesn't seem to be any systematic variation in that number or in any of the numbers that were shown, with perhaps the exception of the velocity. But in terms of torque on the sun, I think the systematic errors which look to be as much as $3°$ means that any calculation of momentum is fruitless.

E. N. Parker Isn't it true that if you were to plot the logarithm of the density and logarithm of the velocity you would get rid of most of that skewness, which pertains to the question of whether the product is more nearly constant.

J. H. Wolfe I think that is probably so.

E. N. Parker The percentage changes I think are not skewed.

J. H. Wolfe Their product is not a constant value.

A. J. Hundhausen I have a few comments that I hope you will find are restrained and positive. Let's start with the solar cycle effects. In a paper recently published in the *Journal of Geophysical Research* Gosling, Hansen, and Bame combined the data from all these different satellites, displaying histograms and giving averages for all the years up to, I think, 1969 or 1970, to get a very similar result. It's very interesting that the highest

velocities were observed near the end of the last solar cycle. There then seems to have been very little change in the yearly average flow speed through the present solar cycle. I think one should emphasize this. In yesterday's discussions of magnetic sectors, changes in the solar wind speed during the solar cycle were evoked. This change doesn't seem to be observed.

Now, considering that decrease in the Vela 2 solar rotation averages of the velocity at or near the very end of the last solar cycle, recall that although something like October-November of 1964 was defined as the beginning of the present cycle, the steady sector pattern observed back in 1963 by IMP 1 appeared to persist until early 1965. In a paper presented yesterday I pointed out that the apparent variations in solar wind density and flow speed with heliographic latitude also appear to begin in early 1965. The new solar cycle may, in fact, have become manifest in the solar wind 6 months after the change in the sunspot pattern.

Finally, with regard to the Vela 3 observations of possible heliographic latitude dependence, the Pioneer 6 and 7 averages and histograms presented here—which I think came from only one or two solar rotations—agree very well with the data I showed yesterday. This limited comparison may not completely confirm the latitude effects, but if this comparison were carried out as Pioneer 6 and 7 get farther from the earth, we would have an independent check as to whether we are seeing latitude effects, time variations, or some instrumental effect.

J. H. Wolfe I think in the last few figures I showed that what Gosling had done could be interpreted either way.

L. Davis, Jr. You spoke of westerly flow and sometimes it sounded as though you were saying from the west. When you say westerly flow do you mean flow *to* the west or *from* the west?

J. H. Wolfe From the west and westerly flow are synonymous. Solar wind people are like weathermen, they talk about the direction from which the wind blows.

R. Lüst From this we get that "negative" would be in conformity with corotation and "positive" against corotation.

J. H. Wolfe With one exception. At MIT they define it the other way around.

Unidentified Speaker You made a point about the raggedness of the velocity distributions and the peak nature. In our experience those peaks usually occur because of the energy channels in the instrument rather than anything occurring in the solar wind.

J. H. Wolfe We questioned those peaks on the Pioneer 7, because they were so ragged, and it just didn't make any sense at all with regard to where the channels were. Certainly I think by the time you get nearly to 5000 points, in the histogram, as we had in Pioneer 6, such instrumental effects tend to go away.

Dr. Newkirk I'm very perplexed by the lack of any change in the condition of the solar wind over the solar cycle. We do see a significant change in the inner corona. The temperature during sunspot maxima is 30 or 40 percent higher; the densities on the average are a factor of 2 higher. These are averages which are constructed differently from those observed in interplanetary space. But we still see an effect as was pointed out by Jack Gosling and his collaborators in their recent paper.

J. H. Wolfe If you are perplexed, then I feel my lecture has been successful this morning. I think we here at Asilomar should discuss current problems and I think the absence of change through the solar cycle is indeed a problem.

N. F. Ness I was a bit puzzled about the emphasis you gave to this comparison between Pioneer 6 and 7 data based upon these snapshots of plasma presented in the NOAA Geophysical Data Series. If I understand the data that are deposited there correctly, they are something like a 1-minute picture of peak velocity for each 24-hour time interval. And when you attempt to compare on short time scales, 1 day or 2 days in the vicinity of the earth, such small segments of data I wouldn't be at all surprised if, even on

the same spacecraft with different time intervals, you would get a scatter diagram. I don't understand why you emphasize that those results substantiate a variable solar wind on such a small time scale. In fact, it would seem to me that we can predict on the order of a few days within the vicinity of the earth if we take the right parameter set. Do you have a comment?

J. H. Wolfe Yes. I think Gosling went through a fairly extended argument in the paper. I'm just showing a list of the conclusions. Actually, the data are from both MIT and ARC. The data from both seem to agree even though they might have been taken at slightly different times. With regard to the snapshot, the number that the project office gives to Virginia Lincoln is a number that best represents that day. The exact time of the measurement is also given. So there's not a 24 hour uncertainty; you know precisely when it was taken. I think Gosling calculated a time at the other spacecraft based on the corotation delay predicted, and compared those two. I think this sort of thing should be done in greater detail with much better data. So I think your point is well taken. But I think the work Gosling did is valid.

D. S. Intriligator I would like to comment on Norman's question. We looked at four solar rotations, two from Pioneer 6 and two from Pioneer 7. We checked this single daily value. We assumed it would not be representative, but we found that instead, on the average, it differed by only 10 percent from the daily average value.

Looking at Pioneer 6 and 7 data from December 1965 to the middle of 1968, we find variations in the number density and velocity that seem to correlate with heliographic latitude.

P. J. Coleman, Jr. I would like to suggest that possibly this is another latitude effect because when spacecraft are separated by 4 or 5 days of corotation time they are separated by something like 6°, since both are in the ecliptic plane.

J. H. Wolfe Agreed. I said there were two explanations, one that the part of the corona which drives the solar wind can evolve in times like 4 days, and the other that these parameters are sensitive to latitude. Those are the two explanations Gosling gave.

J. T. Gosling There are both possibilities. I hope to give a talk after the coffee break where I'll explain a little more, but I think it's primarily a temporal effect.

A. Hundhausen I would like to comment on Gordon's question regarding solar activity. We do see more manifestations of solar activity in the solar wind as the solar cycle progresses. However, these manifestations never seem to dominate the transport of energy (or mass) in the solar wind. For instance, individual flare-produced shock waves appear to be an order of magnitude more energetic 2 years after the solar cycle began than at solar minimum. But there are not very many more such shocks, so that the increased activity doesn't influence the characteristics of the solar wind as greatly as one might expect. However, these activity-related solar wind disturbances do have a more subtle effect, as suggested in a comment made yesterday by Ed Smith. In many ways the *averages* we publish *are* dominated by the presence of these transient and spatial structures. In particular, the compression at the front of a high speed stream has been emphasized here today. This was recognized as early as 1962 in Neugebauer and Snyder's discussions of Mariner 2 observations. But I think few people have looked closely enough at solar wind observations to realize that a very broad rarefaction often follows this compression. When one averages over time, this rarefaction dominates. The density is low at high velocities because of the presence of this rarefaction. It is a *dynamic* effect. Those attempts, mentioned by Gene Parker, to explain such relationships, as the temperature-velocity relationship, by using steady-state models miss entirely this basic dynamic nature of solar wind variations.

J. Hirshberg I wanted to make two points suggesting caution in interpreting the data about the solar cycle. One is about the data on the changes in the velocity. The K_p indices show that the flight of Mariner 2 occurred during a very active period, not at all

typical of the low part of the solar cycle. The other comment concerns the sector structure. We've been saying that the sector structure was constant during the low part of the solar cycle. But the actual data, without the interpolations on the basis of the K_p, contain practically no evidence for this as far as I can see. In the early periods the interpolation using K_p looked good. However, if you do that same thing later on when you have the rapidly changing sector structure the interpolation would not work. So I wonder whether we don't need more data. This is another reason to take measurements continously, that is to get the sector structure through the last half of a cycle.

K. H. Schatten Parker said that the solar wind might not be radial and then Wolfe showed observations suggesting it is. However, I think that Wolfe's observations don't necessarily prove it is radial. There is a large amount of scatter present. If the scatter were related to solar latitude, insofar as the ecliptic is half the time above the solar equator and half the time below it, skewing of the flow could occur and the flow would not be radial although it would appear so from Wolfe's observations.

M. M. Neugebauer I think there's a possibility of systematic error in velocity measurements made from earth satellites. We have noticed such an effect in our OGO data. The maximum pressure in the front of a high velocity stream occurs when the velocity is still relatively low. On several occasions we observed the start of a high velocity stream when OGO-5 was in the solar wind; the velocity started to increase and the density was very high. Then the density dropped, the earth's bow shock moved outward, and OGO was not in the solar wind to observe the highest velocity plasma, which could be seen by deep space probes such as Pioneer 9. In John Wolfe's tables of velocity from all the different spacecraft, you will notice that the average velocity was higher at the deep space probes than at the satellites. So I think there may be a systematic effect here; that is, most of the satellites miss the high velocity periods because the bow shock moves out.

COMMENTS

D. S. Intriligator I would like to elaborate on the comment by M. Neugebauer on a possible systematic bias toward lower velocities in plasma data from spacecraft that are earth orbiters. Figure 1 is from a study Neugebauer and I have been doing to look for a radial gradient affecting the solar wind plasma between 0.75 and 1 AU. We have been comparing simultaneous Pioneer 9 and OGO-5 data. The data in figure 1 are from January 24, 25, 1969. OGO-5 is in earth orbit and is located close to the earth. At this time Pioneer 9 is essentially directly in front of the earth at a radial distance of 0.88 AU. The distance between the two spacecraft is, therefore, approximately 16,000,000 km. As indicated on the abscissa there is almost a 12 hr lag between the Pioneer 9 and OGO-5 data. The darker curves are the OGO-5 data and the lighter curves are the Pioneer 9 data. The bottom graph shows the solar wind velocity recorded at each spacecraft. The two curves follow well until there is a jump in velocity observed at Pioneer 9 at ∼1800 on January 24. Subsequently, at ∼0500 on January 25, OGO-5 was then in the magnetosphere and did not measure this initial interval of higher variations in velocity. There were also several shorter intervals (e.g. ∼1200 on January 25) when OGO-5 was in the magnetosphere during a solar wind velocity increase. At ∼1200 on January 25 Pioneer 9 recorded an extremely large velocity increase and the velocity remained elevated for more than the next 18 hr as shown at the far right of the figure. The initial velocity increase was seen at OGO-5 at ∼2300 on January 25 when the magnetosphere boundary overtook the spacecraft. For more than the next 18 hr OGO was in the magnetosphere. The top graph shows the relative proton flux $(n_p V)$. The OGO-5 data display the total proton flux. The Pioneer 9 data indicate the proton flux in the peak energy channel. The two curves have been arbitrarily displaced. The two curves together show that at ∼1800 January 24 (Pioneer 9) the flux in the peak energy channel increased. At OGO-5 the total flux most likely dropped suddenly and, therefore, OGO-5 was thrown
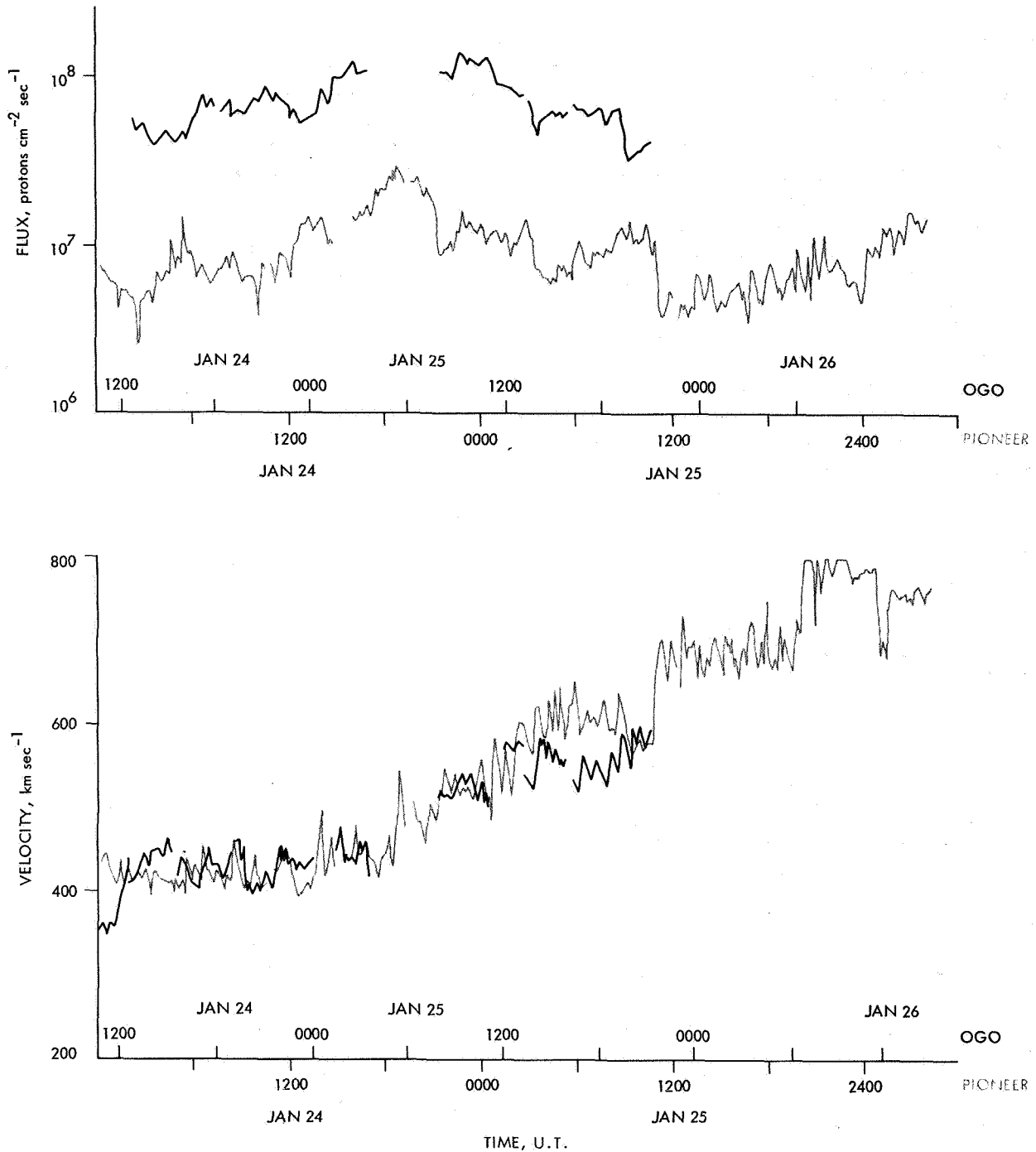
Figure 1. *Simultaneous Pioneer 9 and OGO-5 data from January 24, 25, 1969. The darker curves are the OGO-5 data and the lighter curves are the Pioneer 9 data. The spacecraft are separated by ~16,000,000 km and there is approximately a 12-hr lag time (as indicated on the abscissa) between the event as seen at the two spacecraft. In the top graph the OGO-5 data are the total proton flux and the Pioneer 9 data are the proton flux in the peak energy channel. The two curves have been arbitrarily displaced. The bottom graph indicates the solar wind velocity measured at each spacecraft. Notice the two longer intervals starting at ~1800 Jan. 24 (Pioneer 9 time) and at ~1200 Jan. 25 (Pioneer 9) when the solar wind velocity increases at Pioneer 9 and OGO-5 enters the magnetosphere. The figure shows (see text) that a sharp increase in solar wind velocity and/or a decrease in solar wind flux causes the magnetosphere to expand so that OGO-5 enters the magnetosphere. There is a definite bias in the OGO-5 data toward intervals of lower solar wind velocity and higher solar wind flux.*

200

into the magnetosphere. At ~1200 January 25 (Pioneer 9 time) the peak flux at Pioneer 9 fell sharply. The total solar wind proton flux in the vicinity of the earth probably dropped suddenly at the time OGO-5 reentered the magnetosphere.

These are not unusual events. From studying 3-½ months of simultaneous data (November 1968 until mid February 1969) we find there are many examples of solar wind velocity increases accompanied by simultaneous decreases in solar wind flux. During many of these intervals OGO-5 is overtaken by the magnetosphere and is no longer in the interplanetary medium. There is a definite bias in the OGO-5 interplanetary data toward both intervals of lower solar wind velocity and higher solar wind flux.

DISCUSSION

K. H. Schatten Are you trying to say that the reduced solar wind flux causes the bow shock and magnetopause to move farther out and that's why OGO is in the magnetosphere?

D. S. Intriligator That's right, the bow shock is sensitive to the pressure on it and it moves correspondingly.

E. J. Smith In a way I suppose the comment I want to make is a word of caution. Obviously the stream-stream interactions are very important and there are many cases, some of which have been shown today, in which you see the effects of a pileup of the plasma ahead of the solar wind stream. But just to try and provide what I consider to be some balance to the presentation, there are other cases in interplanetary data in which you see rather large increases in the plasma density which are probably not due to any sort of pileup. In particular, there are the increases in the density that occur near the minimum of the solar wind speed. These happen to be the portions of the solar wind in which one is likely to find sector boundaries. If you look only at the plasma data you may not be able to distinguish readily whether the higher density is due to a pileup or not. If you look at the magnetic field data, you will see that during those occurrences the magnetic field magnitude does *not* increase, whereas in regions where there is compression or pileup taking place the magnetic field magnitude should increase along with the density of the plasma. Another difference is that these density increases occur well ahead of the positive gradient regions. There is a substantial delay because the solar wind streams and the high velocity streams, tend to be fairly narrow and that leads to fairly broad valleys or minima in the velocity. It's in these minima that this type of density increase occurs. The increases are then presumably related to something having to do with the origin of that portion of the solar wind, and are not likely to be the result of some kind of stream-stream interaction.

Finally, I might just mention that it's these broad valleys of lower velocity and narrow peaks of higher velocity that cause skewness in many of the histograms that were shown today. A high velocity stream is present for a very short period of time; consequently, you have fewer samples. On the other hand, low velocity regions usually last longer because they are broader in spatial extent, and you get a lot of readings.